FERMILAB-PUB-83-72

Fermilab Dedicated Collider

II. PHYSICS OPPORTUNITIES

J.Bjorken, E. Eichten and C.Quigg

The conventional possibilities for collider physics have been spelled out in many places, most recently in the 1982 Snowmass Workshop. Although these are unlikely to represent the most far-reaching results to be obtained with the Dedicated Collider, they provide useful benchmarks for assessing the sensitivity and richness of a new facility. In this brief chapter, we show how the Dedicated Collider responds to the expected physics. We also show how the DC opens a new and important energy regime, and indicate the unique potential of this device for dramatic experimental progress.

A. Beyond the Bellwethers

The spectacular results from $S\bar{p}pS$ experiments UA1 and UA2 are important not only for their direct contributions to science, but also for what they portend for future facilities. They demonstrate that:

1. $\bar{p}p$ colliders work. Intense antiproton sources of good emittance can be built. The beam-beam interactions are (at worst) no more disruptive than anticipated.

2. Hard collisions occur in hadron-hadron interactions. The theoretical rate projections have been reasonably accurate, and extraction of signals from background has not been any more difficult than generally anticipated. Indeed, those who felt that a very high integrated luminosity would be required to extract the signal for the leptonic decay of the W were unprepared for the convincing evidence for the intermediate boson that emerged from only a few events.

3. Multijet events are manifestly analyzable. The striking LEGO plots of these events promise a rich future for fine-grained calorimetric techniques for identifying and measuring electromagnetic and hadronic jets. One can well imagine the measurement of inclusive spectra of jets and leptons becoming relatively pedestrian as techniques of multijet spectroscopy mature. We may already anticipate relatively strong statements from the next $S\bar{p}pS$ running period on the existence of the top (or other) quark(s) in the mass range of 20-60 GeV/c , based on the measurement of two or more particles (or jets) per event. These multijet phenomena are likely to dominate experimental and theoretical attention within the next few years, and certainly in the time frame we consider here for the DC. The mastery of multijet spectroscopy will liberate us from reliance upon low-branching-ratio signatures for interesting new phenomena. One must also bear in mind that the c.m. energy of the DC is more than seven times greater and the luminosity more than 200 times greater than what is now available at the $S\bar{p}pS$.

An important element of the Dedicated Collider complex is a high-luminosity electron-proton collider. Initially projected for 10

Appeared as Chapter 2 of Proposal for a Dedicated Collider at Fermi National Accelerator Laboratory, May 1983

GeV × 2 TeV operation, this facility has significant growth potential, since a 40 GeV electron ring can be accommodated in the DC tunnel. In the initial phase, the DC electron option is competitive with the proposed HERA machine. In its second stage, the DC ep collider is unique in the world.

In what follows we survey the physics opportunities presented by the Dedicated Collider. We proceed from the conventional features implied by the standard model to more speculative topics, and close the pp discussion with a very brief general discussion of the rates for hard collisions among partons, along with a discussion of the limitations of the calculations.

We then turn to an outline of the DC's capabilities for electron-proton physics. Again this topic has been the subject of many proposals and summer studies, so we shall content ourselves with a discussion of the main points. Although an ep collider has not been built before, the virtues of ep collisions are well appreciated. The electron provides a well understood and apparently structureless probe, and the ep facility nicely complements the existing and projected e^+e^- and hadron-hadron (i.e., quark-quark) colliders. ep collisions are particularly sensitive to deviations from the standard model; right-handed currents, quark substructure, lepton-quark compositeness contact term, and clean signatures for heavy quark (or leptoquark) production. These opportunities for discovery are examined in Section G of this chapter.

B. Electroweak Phenomena

The discovery of the intermediate boson establishes, as expected, the 100 GeV regime of c.m. energy as the natural scale of the electroweak interactions. The SppS and Tev I programs, and especially the LEP and SLC electron-positron colliders, should provide a rather thorough exploration of this energy regime. In addition, TeV I will make possible the first look beyond this energy scale. As already mentioned, the natural habitat of the DC is in the realm of hard-collision invariant masses between 0.5 and 1 TeV. This is not to say that conventional electroweak/QCD physics will be neglected, however.

As an example, we show in Table II-1 the number of standard model intermediate bosons to be expected in a standard run (integrated luminosity $\int \mathcal{L} dt = 10^{38}\ cm^{-2}$) at the DC. The expected number is of order 10^6, which should be large enough to permit many detailed studies. This represents a significant increase over the rates anticipated for the SppS and TeV I, and is also competitive with what might be achieved in a high-luminosity CBA. For the neutral gauge bosons Z^0 the e^+e^- colliders would seem to retain a decided advantage in event rate.

The situation is similar for the production of pairs of gauge bosons, a measurement which provides some of the motivation for LEP II.

The cross section is sensitive to three-gauge-boson couplings, and has been advocated as a test of the non-Abelian nature of the interaction. Whether it will in fact be the most sensitive test remains to be seen. In any case, as shown in Table II-2, the DC will produce these events in interesting numbers. The cross section for the related $W\gamma$ final state, which is sensitive to the magnetic moment of the intermediate boson, is strongly dependent on the cut imposed upon the photon momentum. The anticipated event rate is typically greater than or equal to the pair production rates in Table II-2.

Within the standard model, the spontaneous symmetry breaking is accomplished by an elementary scalar Higgs boson. The mass of the Higgs boson is an arbitrary parameter of the theory as it is currently understood, subject only to the bounds

$$7.4\ \text{GeV}/c^2 < M_H \lesssim 1\ \text{TeV}/c^2.$$

It is plausible that the upper bound, which is based on the consistency of perturbation theory, can be improved to approximately 400 GeV/c^2. If $M_H \lesssim 40$ GeV/c^2, it should be possible to detect the Higgs boson in Z^0 decays at SLC or LEP. LEP II could perhaps extend the limit to about 100 GeV/c^2 in the process

$$e^+e^- \rightarrow H + Z^0.$$

The DC is sensitive to still higher masses. The production mechanism of $gg \rightarrow H$ via a fermion triangle is sensitive to the mass of the top quark, as shown in Fig. II-1. Table II-3 shows the highest Higgs boson mass for which 100 events will be produced for the benchmark luminosities. For Higgs masses in excess of about $2M_W$, the dominant decay mode will be into pairs of gauge bosons. This would provide a characteristic signature for hadron-jet spectroscopy. The mass range $M_W < M_H < 2M_W$ is more problematic, and may require good luck--or an e^+e^- collider.

Should the top quark be very heavy, or should a fourth fermion generation exist, it is of interest to search for heavy quarks using the methods now being evolved at the $S\bar{p}pS$. Pair production cross sections estimated from the gluon fusion mechanism are shown in Fig. II-2. The DC again considerably extends the range of accessible masses, as summarized in Table II-4.

A simple extension of the standard model would entail the existence of additional gauge bosons. In the case of a right-handed W-boson, which would restore left-right symmetry at high energies, the ep facility of the Dedicated Collider would be an important diagnostic tool. Couplings of additional gauge bosons to the light fermions are evidently model dependent, but reasonable cross section estimates for production in $p\bar{p}$ collisions may be had by assuming universality of the

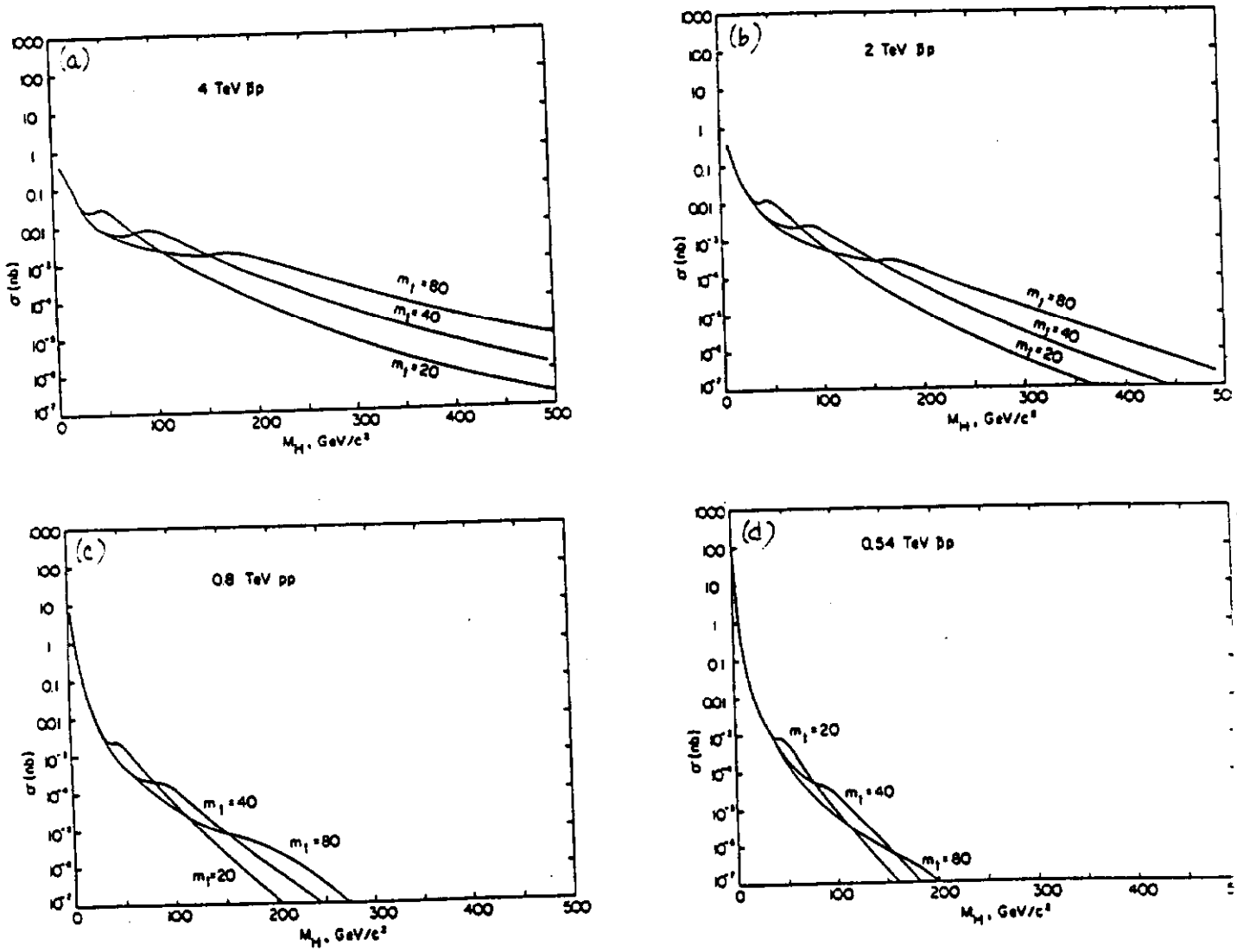

Fig. II-1. Cross sections for production of Higgs bosons in hadron-hadron collisions. (a) 4 TeV $\bar{p}p$; (b) 2 TeV $\bar{p}p$; (c) 0.8 TeV pp; (d) 0.54 TeV $\bar{p}p$.

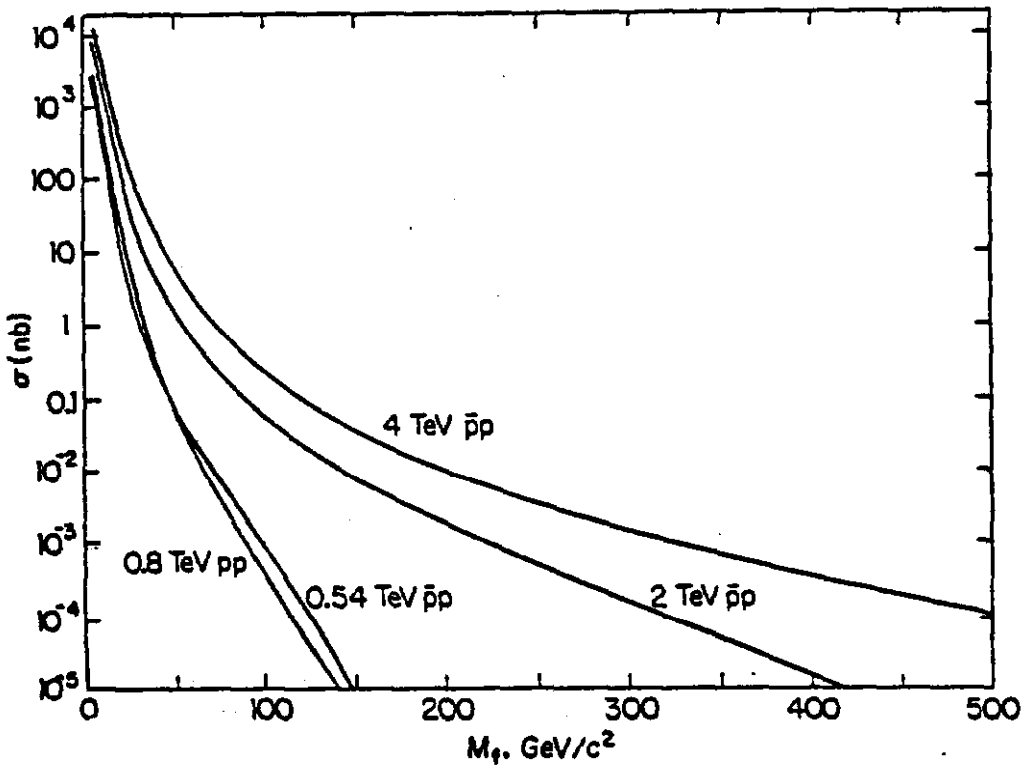

Fig. II-2. Cross sections for production of heavy quark pairs in hadron-hadron collisions.

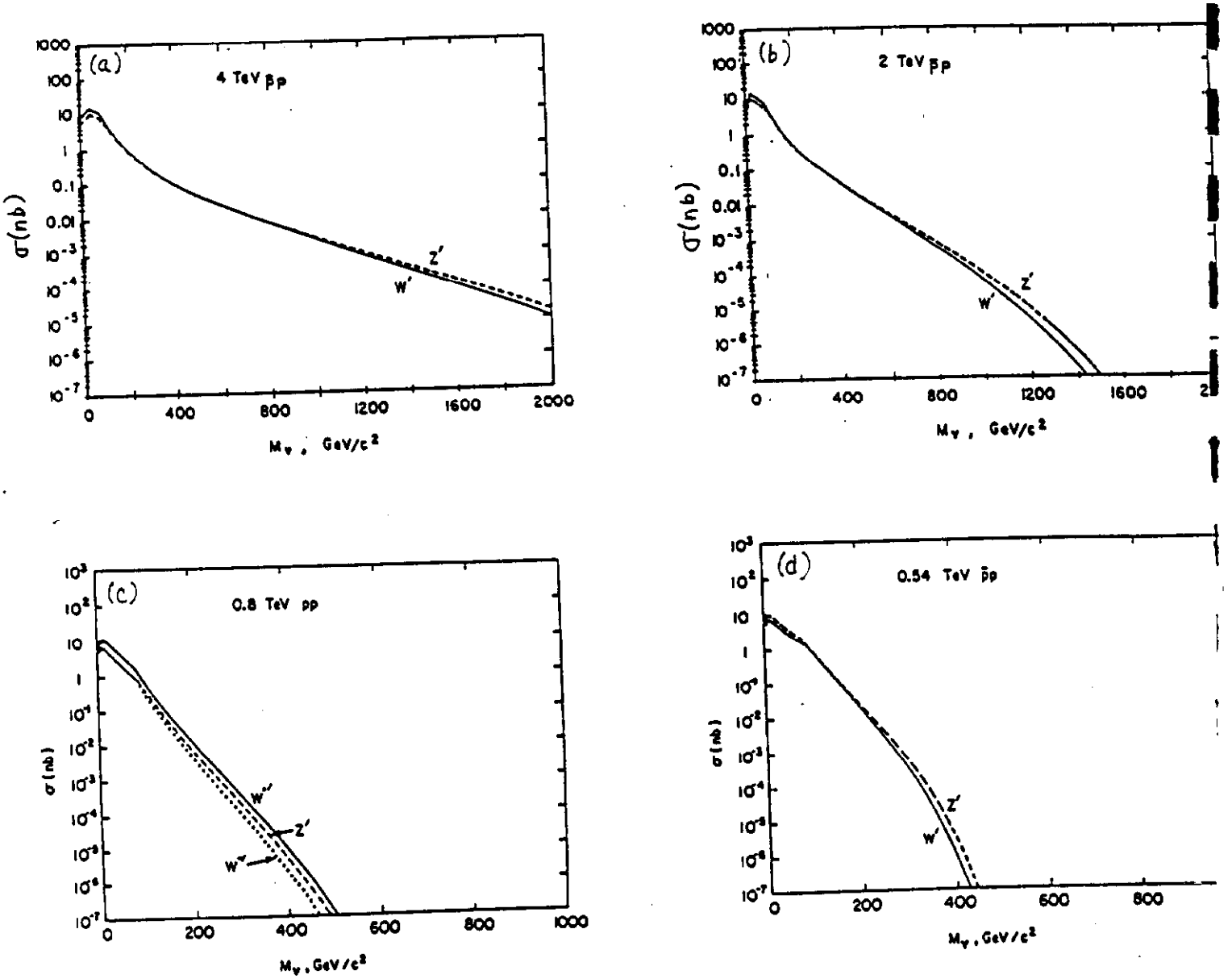

Fig. II-3. Cross sections for production of heavy electroweak gauge bosons in hadron-hadron collisions. (a) 4 TeV $\bar{p}p$; (b) 2 TeV $\bar{p}p$; (c) 0.8 TeV pp; (d) 0.54 TeV $\bar{p}p$.

gauge couplings. Cross sections computed on this basis are displayed in Fig. II-3. The highest masses for which 100 events are produced are tabulated in Table II-5. The DC sensitivity extends well beyond 1 TeV/c^2.

In the context of the DC scale of subenergies, dilepton production does not appear especially interesting for its own sake. Nevertheless, as Fig. II-4 shows, there is sensitivity at the level of one event per GeV/c^2 in $d\sigma/dM$ out to an invariant mass of approximately 250 GeV/c^2.

C. Hadron Jets

Early running at the CERN $S\bar{p}pS$ has confirmed the expectation that the cross sections for hard scattering of constituents are large. Moreover, LEGO displays of the kind included as Fig. II-5 have shown that for an important class of events the jets are well collimated, isolated, and straightforward to analyze. Already in limited running, hard collisions have been observed at c.m. energies in excess of those that may be attained in e^+e^- collisions for a decade or more.

Jet studies in hadron-hadron collisions have traditionally been viewed as less incisive than those carried out in electron-positron annihilations or in lepton-nucleon scattering because of the added complexity of events. The $S\bar{p}pS$ experience indicates that, as hoped, the hard scattering events take on a much simpler aspect at high energies, and there is no impediment to detailed analyses. We may therefore expect to take advantage of the higher energies attainable in hadron-hadron collisions and of the greater diversity of elementary interactions made possible by our unseparated broad-band parton beams.

To give an indication of the expected cross sections, we show in Fig. II-6 the lowest-order QCD hard-scattering contributions to $d\sigma/dydp_T$ at 90° in the c.m. Our current understanding of QCD seems not to justify a more elaborate calculation. In any event, the prediction for $\sqrt{s} = 0.54$ TeV is in reasonable agreement with the preliminary data from the UA1 experiment. One may read off, as a figure of merit, the maximum (single-jet) transverse momentum for which a standard run will yield 100 events per bin of 1 unit of rapidity and 1 GeV/c of transverse momentum, i.e., the point at which

$$\int dt \mathcal{L} \cdot \left.\frac{d^2\sigma}{dydp}\right|_{y=0} = 100/(\text{GeV}/c).$$

These values of p_T are collected in Table II-5. At the Dedicated Collider, one can anticipate extensive studies of hadron jet phenomena for jet transverse momenta in excess of 350 GeV/c, corresponding to elementary collisions at $\sqrt{s}$ ~700 GeV. Exploratory studies will be possible to considerably higher transverse momenta.

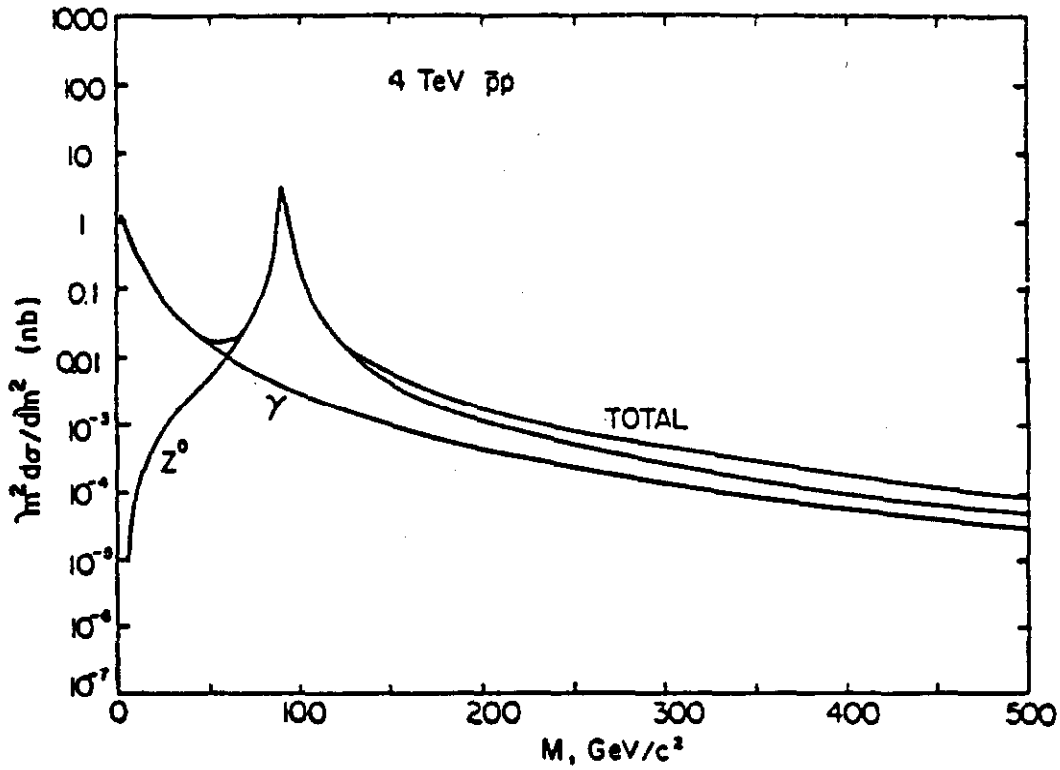

Fig. II-4. Differential cross section $m^2 d\sigma/dm^2$ for production of massive lepton pairs in 4 TeV $\bar{p}p$ collisions.

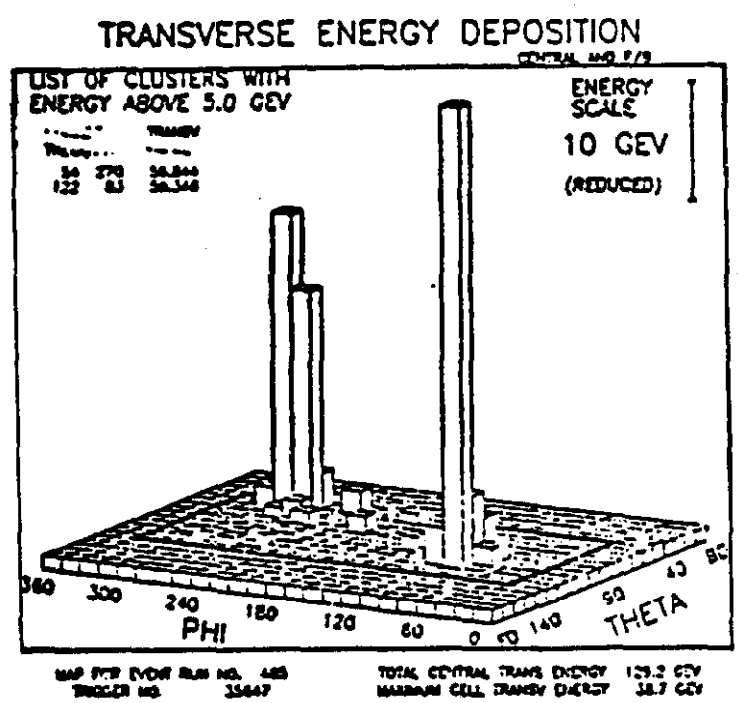

Fig. II-5. "LEGO" display of a typical two-jet event observed in the UA2 detector at the $S\bar{p}pS$.

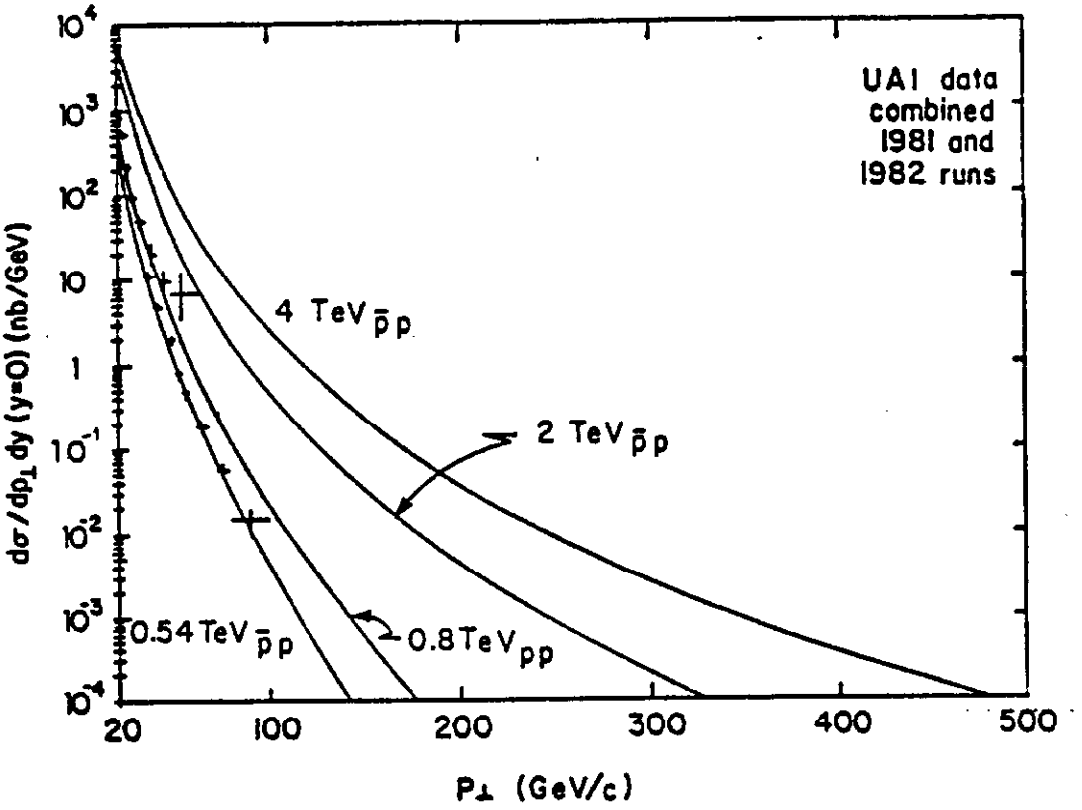

Fig. II-6. Hard scattering contribution to the production of hadron jets at 90° in the c.m. The 1981-1982 UA1 data collected in 0.54 TeV $\bar{p}p$ collisions are shown for reference.

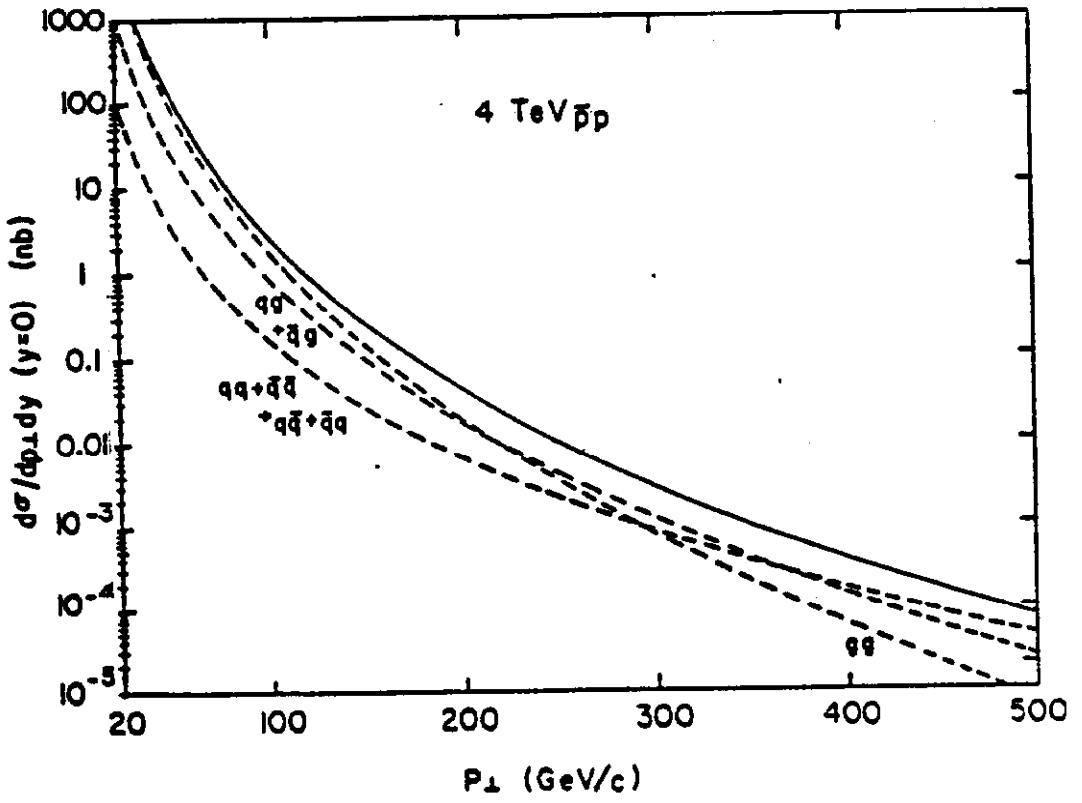

Fig. II-7. Jet production by components in 4 TeV $\bar{p}p$ collisions.

The prospect of studying fully-developed jets is enhanced by the possibility of distinguishing between gluon jets and quark jets by kinematic selections. How this might be done is indicated first in Fig. II-7, which shows separately the contributions to $d^2\sigma/dydp_T$ of the

$$gg \to (gg \text{ and } q\bar{q})$$

$$gq \to gq \text{ and } g\bar{q} \to g\bar{q}$$

$$\begin{cases} qq \to qq \\ \bar{q}\bar{q} \to \bar{q}\bar{q} \\ q\bar{q} \to q\bar{q} \end{cases}$$

processes. Because the cross section for $gg \to q\bar{q}$ is negligible compared to that for $gg \to gg$, these three classes of processes correspond closely to two-gluon, (anti)quark-gluon, and two (anti)quark jets. At modest transverse momenta, of order 100 GeV/c or less, the two-gluon final state is dominant. The mix changes markedly at larger values of p_T, so that quark jets ultimately prevail.

Another method of separation is made possible by the different rapidity dependence of the components. Figures II-8 (a)-(e) show the behavior of

$$\left.\frac{d\sigma}{dp_T\, dy_1 dy_2}\right|_{y_2=-y_1}$$

as a function of y_1 for various fixed values of p_T. The gluon-gluon process prevails at small p_T and small rapidities, while the reactions involving valence quarks become dominant at large p_T and large rapidities. A similar effect is shown in Figs. II-9 (a)-(c), where the transverse momentum of the jet is held fixed at p_T = 200 GeV/c, and the c.m. rapidity $y_B = y_1 + y_2$ of the colliding partons is varied. The possibilities for dramatic changes in the mix of jets are readily apparent.

Interesting as the study of two-jet events may now seem, it may well be rather straightforward and thus rapidly assume the traditional role of Bhabha scattering in e^+e^- colliders: prominent, quickly and accurately measurable, and thereafter neglected by all but the Feynman-diagram computer technologists. Multijet events and multijet spectroscopy would then become the focus of research interests for perturbative QCD in this regime. Again, it is the high energy, diversity of processes, and simplicity of jet spectroscopy which raise our hopes.

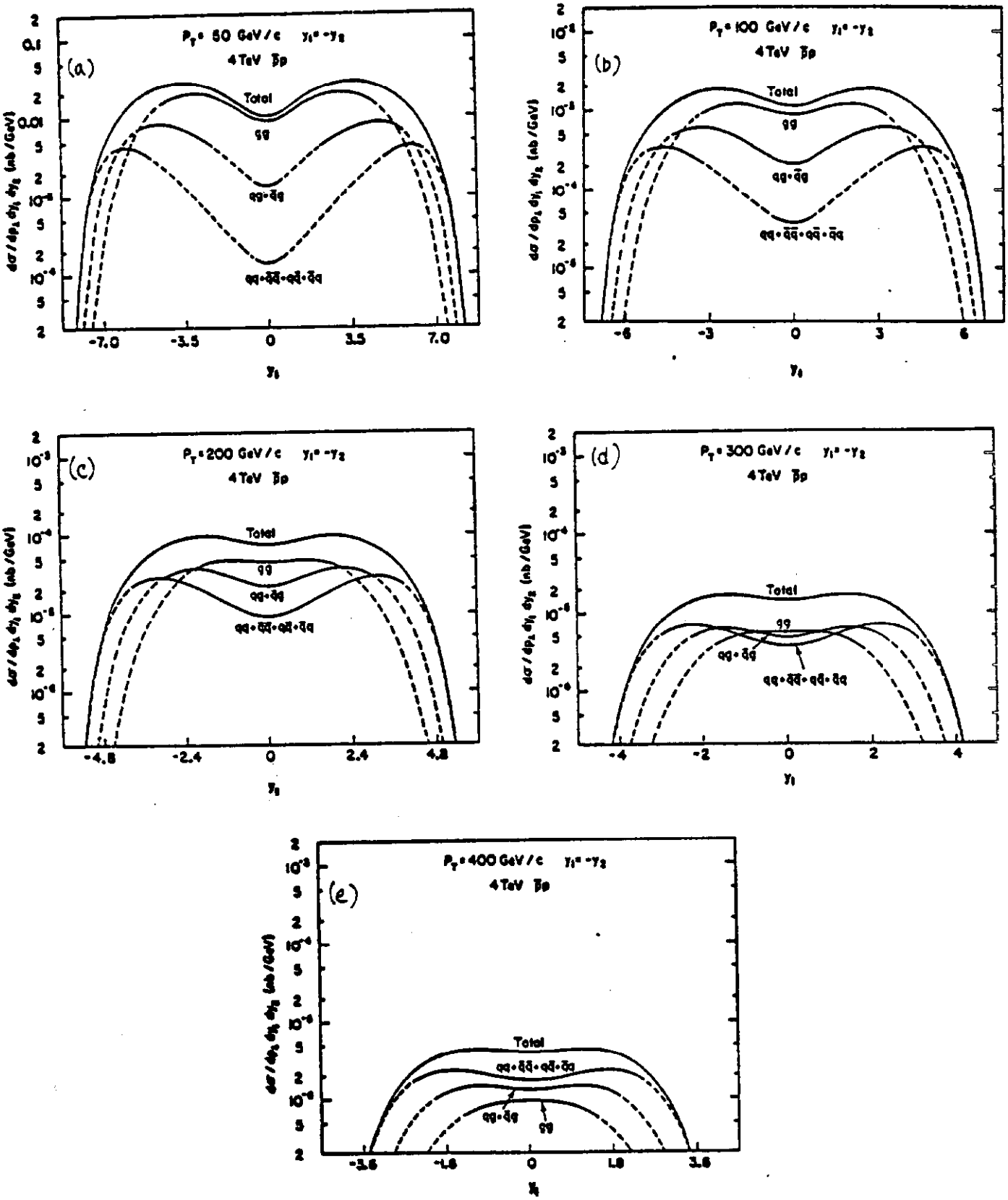

Fig. II-8. Contributions of hard-scattering components to symmetric ($y_1+y_2 = 0$) jet production, for specified transverse momentum of each jet in 4 TeV $\bar{p}p$ collisions. (a) $p_\perp$ = 50 GeV/c; (b) $p_\perp$ = 100 GeV/c; (c) $p_\perp$ = 200 GeV/c; (d) $p_\perp$ = 300 GeV/c; (e) $p_\perp$ = 400 GeV/c.

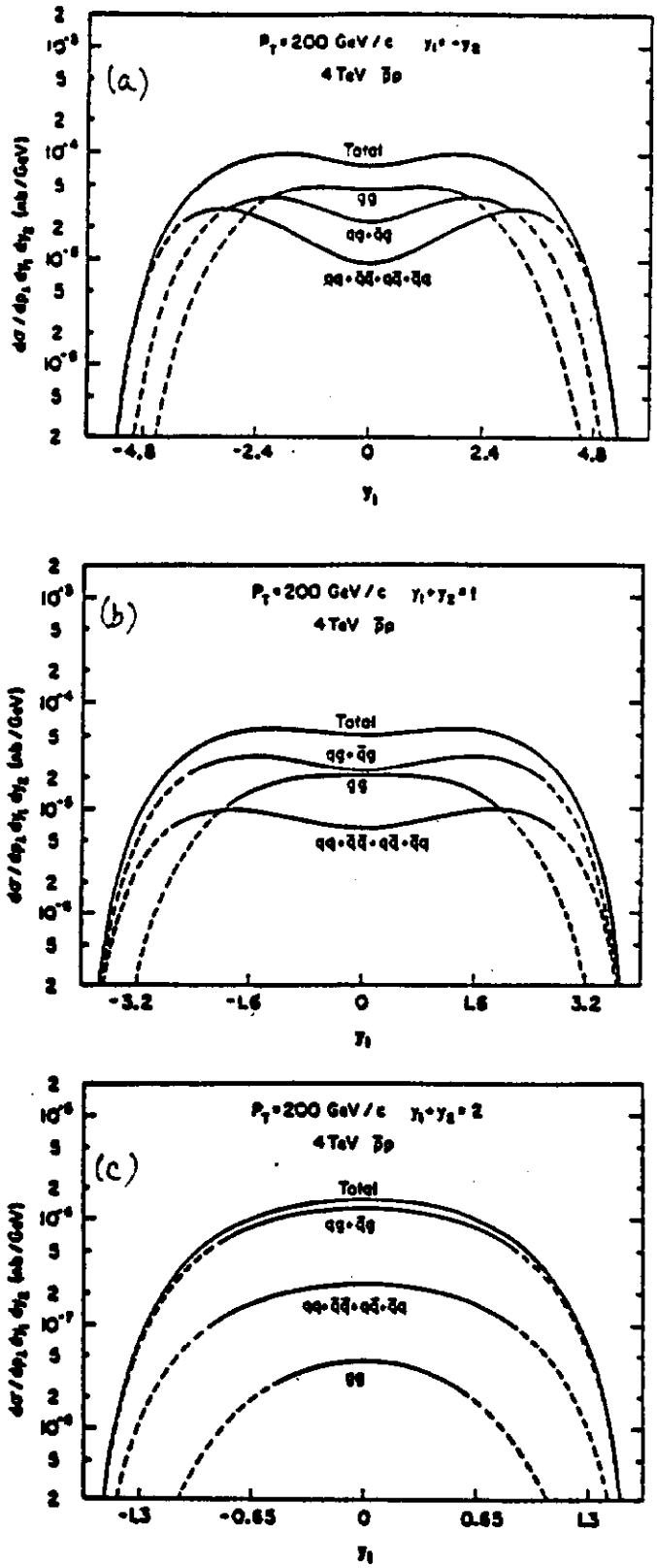

Fig. II-9. Contributions of hard-scattering components to jets of $p_\perp$ = 200 GeV/c, as a function of the rapidity y_1+y_2 of the hard-collision c.m. (a) $y_1 + y_2 = 0$; (b) $y_1 + y_2 = 1$; (c) $y_1 + y_2 = 2$.

D. New Landmarks in 1-TeV Physics

In many ways, the scale of 1 TeV represents the frontier of our ignorance. It describes a regime in which we have, as yet, no direct experimental information and one in which our current understanding seems to compel the existence of new phenomena. The necessity of new physics is more convincing than the argument for any specific manifestation of the new scale, so it is important to explore this region with good sensitivity to many possibilities.

What are the physics landmarks in this regime? The clearest one is given by the fundamental parameter of electroweak spontaneous symmetry breaking, the vacuum expectation value $\langle\phi\rangle_0$ of the Higgs field, which is equal to about 174 GeV. The origin of this scale, which is considerably larger than that of the intermediate bosons, is dimly understood. This alone provides a solid stimulus to the exploration of this regime. Most lines of theoretical speculation have as a primary goal the improved understanding of the dynamics of the Higgs sector. Typical scenarios populate the region between 100 GeV and 10 TeV with a multitude of new particles. In each of the proposed scenarios:

Technicolor
Supersymmetry
Compositeness

there are clearly identifiable signals of this dynamics at energies at or below $G_F^{-1/2} \approx 250$ GeV. Each of these alternatives has a light sector of bosons (and/or fermions) whose existence is associated in a fundamental way to the approximate chiral symmetries at the new interaction scale. This light sector comprises the set of least massive members of the family of new particles and is a general feature of any dynamics at this scale.

In technicolor the light sector is bosonic--the specific new particles have been called technipions--while in the supersymmetric models both bosons (squarks and sleptons) and fermions (gluino, photino,...) result. In composite models the role of the light sector of the theory is provided by some (or all) of the ordinary quarks and leptons. Here, therefore, the signal of the new dynamics will show up directly in the hard scattering of quarks and leptons. We will discuss each of these alternatives in turn.

1. Technicolor

In the standard electroweak theory, the spontaneous symmetry breaking is accomplished by the action of a complex doublet of elementary scalar fields. Subject to constraints imposed by neutral current phenomenology, there may in principle be any number of elementary scalars and the resulting Higgs bosons. How many there are, what are the masses of the surviving physical scalars, and what are their couplings to ordinary matter can only be settled experimentally. The standard theoretical framework offers no guidance, other than rather broad (and nonrigorous) bounds on the Higgs boson mass.

An alternative description goes by the name of dynamical symmetry breaking or, colloquially, technicolor. This program attempts to find a dynamical basis for the Higgs scale in terms of new strong (technicolor) interactions at a scale of about 1 TeV, and thus to explain the breakdown of $SU(2)_L \otimes U(1)_Y \rightarrow U(1)_{EM}$ and the generation of fermion masses. In this approach, spinless bound states of heavy fermion-antifermion pairs play the role of the elementary scalars of the standard model. The lightest of these, dubbed technipions, are the most immediately accessible to experiment.

No phenomenologically acceptable model of dynamical symmetry breaking has been developed, and so many details of the conjectured spectrum are unsettled. The general idea of dynamical symmetry breaking is however so natural and appealing, and the general arguments for structure in the few-hundred GeV regime so compelling, that a careful search is mandatory.

A number of the conjectured composite scalar mesons have appreciable couplings to gluons and hence can be produced copiously in hadron-hadron colliders. The so-called technieta (η_T or P_8) can be produced in two-gluon fusion with the cross sections shown in Fig. II-10. This leads to a sensitivity at the 100 events per run level as shown in Table II-7. For the Dedicated Collider, the maximum accessible mass of 640 GeV/c^2 is well above the "expected" mass of ~240 GeV/c^2. Heavy pairs of colored technihadrons can also be produced, as indicated in Fig. II-11 with (solid curves) and without (dashed curves) the expected technivector meson enhancements. The maximum accessible masses at the DC as shown in Table II-8 are again well above the conjectured values $M(P_3) \sim 160$ GeV/c^2, $M(P_8) \sim 240$ GeV/c^2, $M(P_6) \sim 260$ GeV/c^2. The technihadrons should have distinctive decay signatures involving multiple jets and leptons.

2. Supersymmetric Partners of the Known Particles

A possible sign of the incompleteness of the standard model is the arbitrariness that remains even after a minimal unification of the strong, weak, and electromagnetic interactions. The gauge bosons may be said to be prescribed by the local gauge symmetry, but the elementary fermions are put in by hand, and the elementary scalar fields and their self-interactions are, for now, total invention. The possibility of relating vector, spinor, and scalar particles in a way that reduces or eliminates the unwanted freedom of the model has an obvious appeal. The fermion-boson symmetry known as supersymmetry raises the hope that such a simplification might be achieved. However, it is now apparent that the observed particles cannot be supersymmetric partners of each other. Therefore, if supersymmetry is useful on the present energy scale, it implies a doubling of the spectrum with the following minimal complement of new objects:

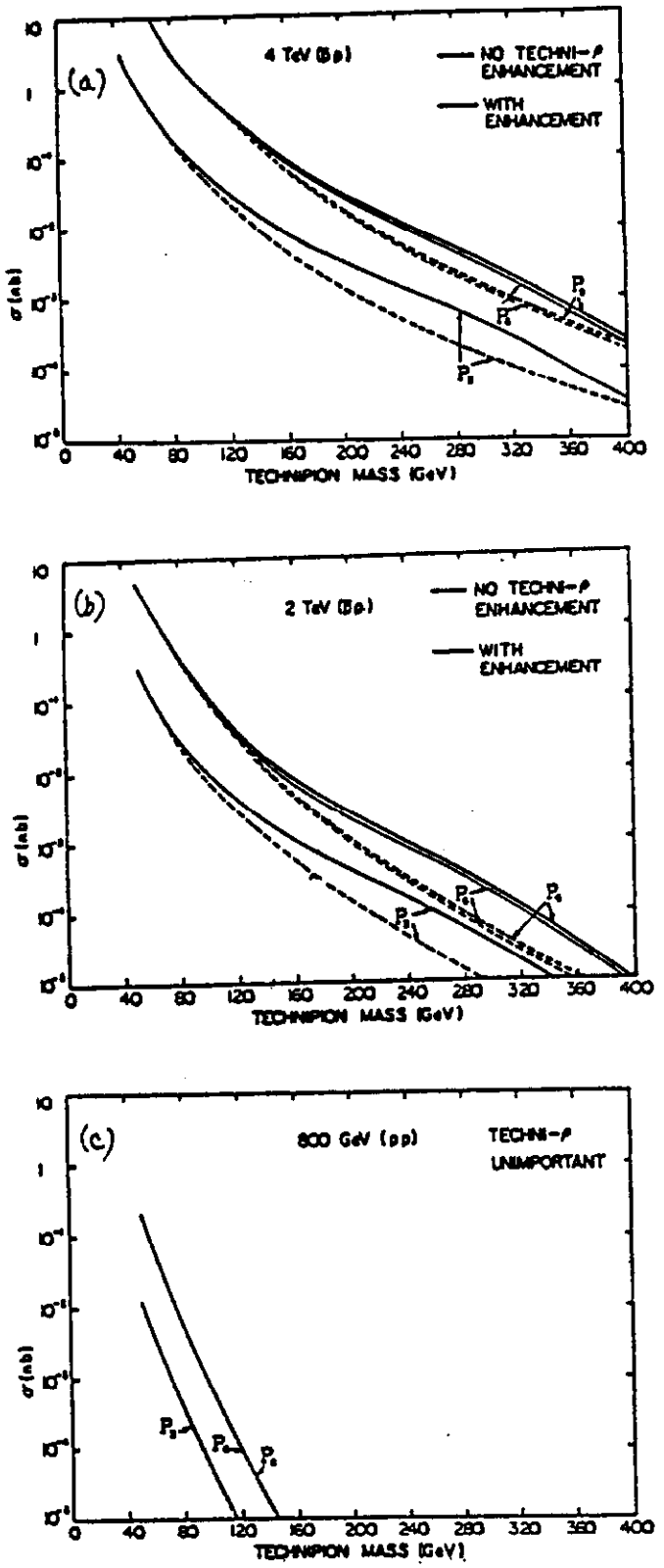

Fig. II-10 . Cross sections for pair production of technipions with (solid curves) and without (dashed curves) technirho enhancement. (a) 4 TeV $\bar{p}p$; (b) 2 TeV $\bar{p}p$; (c) 0.8 TeV pp.

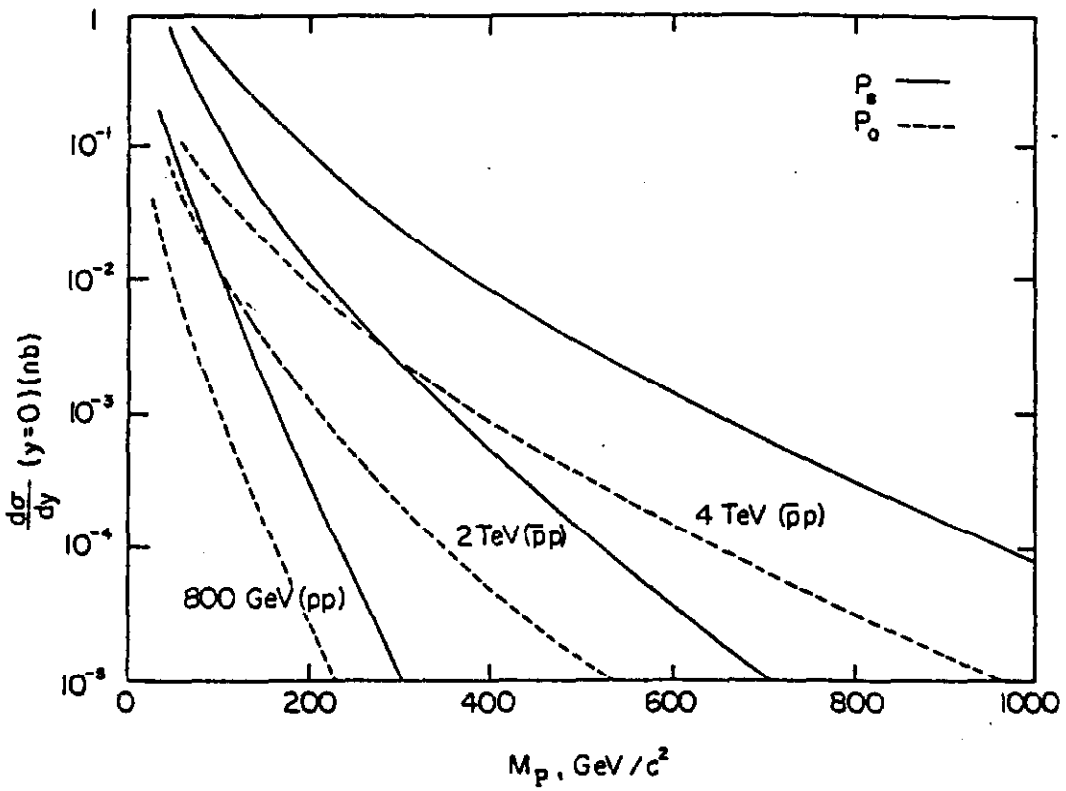

Fig. II-11. Differential cross sections $d\sigma/dy$ ($y = 0$) for production of Higgs-like scalars in hadron-hadron collisions.

Established Particles			Supersymmetric Partners		
J=1	gluons		gluinos $\tilde{g}$		J=1/2
	intermediate bosons	$W^{\pm}$	winos	$\tilde{W}^{\pm}$	
		Z°	zino	$\tilde{Z}$	
	photon γ		photino	$\tilde{\gamma}$	
J=1/2	leptons ℓ		sleptons	$\tilde{\ell}$	J=0
	quarks q		squarks	$\tilde{q}$	
J=0	Higgs boson H		higgsino	$\tilde{H}$	J=1/2

These are plainly not degenerate with the established particles, so supersymmetry must be broken. No convincing model of broken supersymmetry which meets phenomenological requirements has yet been formulated. Consequently the pattern of masses and decay chains of the superparticles is open to speculation. In contrast, the elementary couplings involving superparticles should be related to known couplings by Clebsch-Gordan coefficients.

While worthwhile in its own right, a complete survey of possibilities would be out of proportion to the importance of superparticles to the justification of the DC. The particles which seem to be of greatest interest for a high-energy hadron collider are the colored squarks and gluinos. The cross section for pair production of squarks is shown in Fig. II-12 as a function of squark mass. Under the running conditions anticipated for the DC, the event rate is ample in the 100 GeV/c^2 regime. As Table II-9 shows, the maximum squark mass for production of 100 pairs is approximately 215 GeV/c^2, which exceeds what may be anticipated for other machines.

The expected gluino production rates are still larger, because of the larger color charge of the gluino. These are shown in Fig. II-13 and Table II-10. In this case, the DC should provide sensitivity out to a mass of 400 GeV/c^2.

3. Compositeness

The standard model is based upon the notion that the quarks and leptons are elementary particles, and indeed there is direct experimental evidence that they are structureless on a scale of $\sim 10^{-16}$cm. However, both history and the proliferation of flavors encourage us to consider the possibility that quarks and leptons are themselves composite. The right such model might then predict the spectrum and reduce the arbitrariness inherent in the standard model.

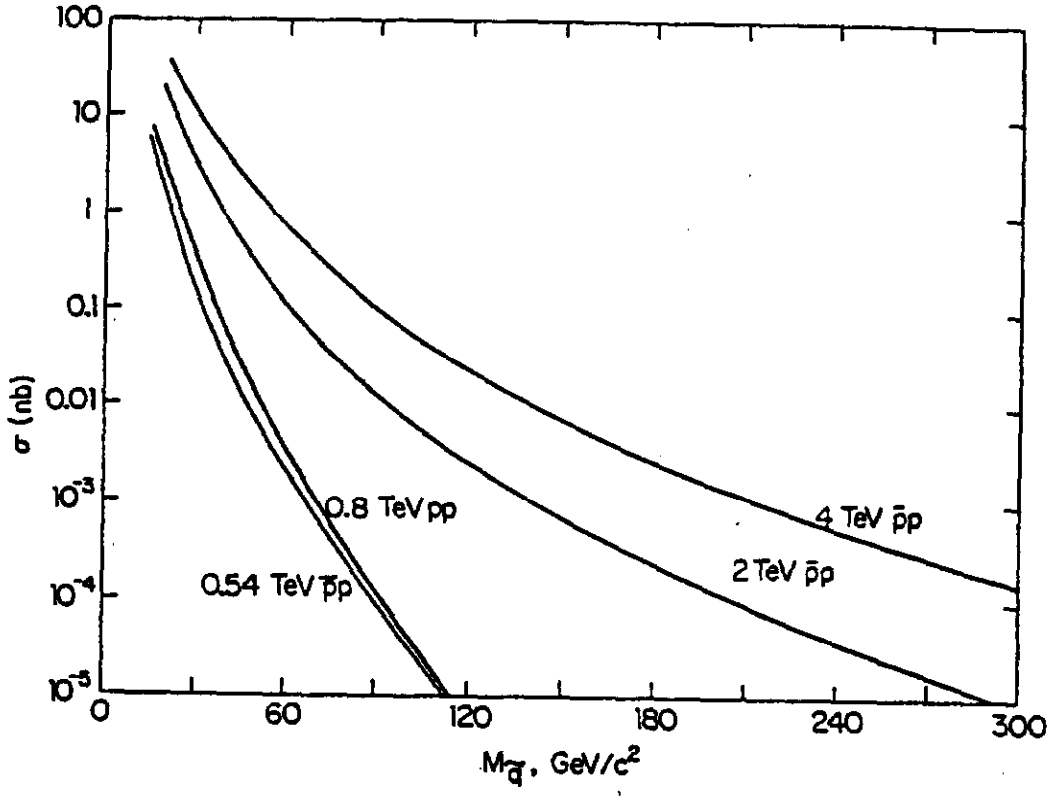

Fig. II-12. Cross sections for pair production of squarks in hadron-hadron collisions.

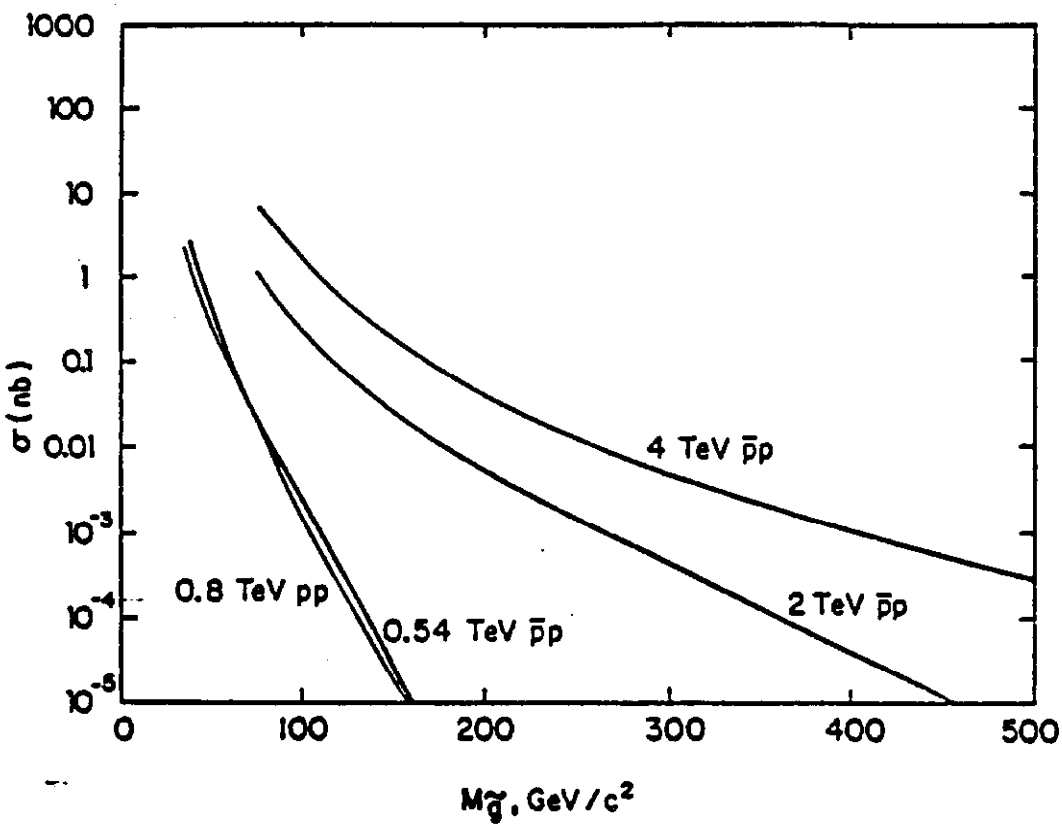

Fig. II-13. Cross sections for pair production of gluinos in hadron-hadron collisions.

One manifestation of compositeness would be the appearance of form factors for the quarks and leptons. While evidence on this point will be accumulated in both the ep and $\bar{p}p$ modes of the DC, another signature may be more telling in the near term. This is the effect of a new contact interaction between quarks and leptons which should emerge if these fermions have constituents.

If quarks and leptons are bound states, the force that binds the constituents will also mediate new interactions among the bound states. At energies far below the compositeness scale, these new interactions may be represented as effective contact terms of the form

$$\delta = \pm\frac{g^2}{\Lambda^2}(\bar{f}f)(\bar{f}'f') ,$$

where Λ is the compositeness scale. It is plausible (since the interactions must be strong) that $g^2/4\pi = 1$.

The effect of the contact term on jet production for various values of Λ and for both + and - signs in the coupling is shown in Fig. II-14. Under the assumption that detection of a departure from QCD expectations would be noticeable if the deviation is (i) by a factor of two or more, (ii) gives at least 100 events/run variation from expectation, and (iii) gives a detectable non-scaling energy behavior, the sensitivity is indicated in Table II-11. It should be possible to observe a compositeness scale of up to 3 TeV at the DC.

If both the light quarks and muons are composite, then the effects of the contact interaction will modify the usual Drell-Yan cross section. The resulting cross sections are shown in Fig. II-15. The maximum compositeness scale to which one may expect to be sensitive is shown in Table II-12, under similar assumptions to those made for the hadron jets. The limit set on Λ by the DC should be 6 TeV.

Finally, there is the possibility in a composite model that excited colored objects may be pair-produced in hadronic collisions. These exotic fermions might be expected to appear with masses of a few hundred GeV/c^2. Table II-13 shows that for color triplets, sextets, and octets the DC provides sensitivity over an interesting range.

E. Parton Luminosities; Summary of $\bar{p}p$ Opportunities

High-mass hard collisions are the principal avenue to high-energy parton-parton interactions. Cross sections for hard collisions are characterized by the limiting high-energy behavior

$$\sigma(\hat{s}) = c/\hat{s},$$

where $\hat{s}$ is the squared subenergy for the elementary process and c is a process-dependent number which typically lies between 10^{-3} and 1. The

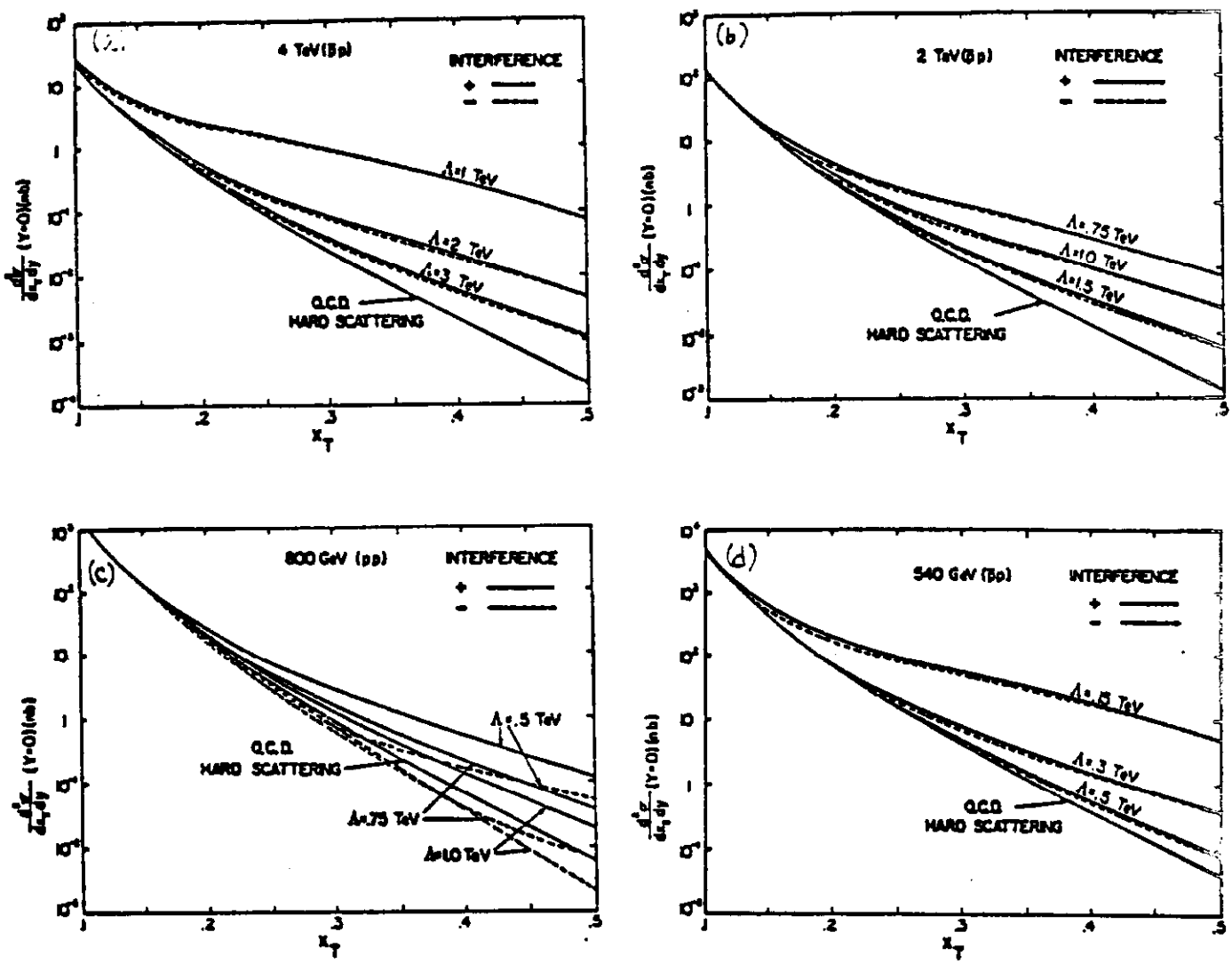

Fig. II-14. Deviations from QCD yields for jet production induced by quark compositeness. (a) 4 TeV $\bar{p}p$; (b) 2 TeV $\bar{p}p$; (c) 0.8 TeV pp; (d) 0.54 TeV $\bar{p}p$.

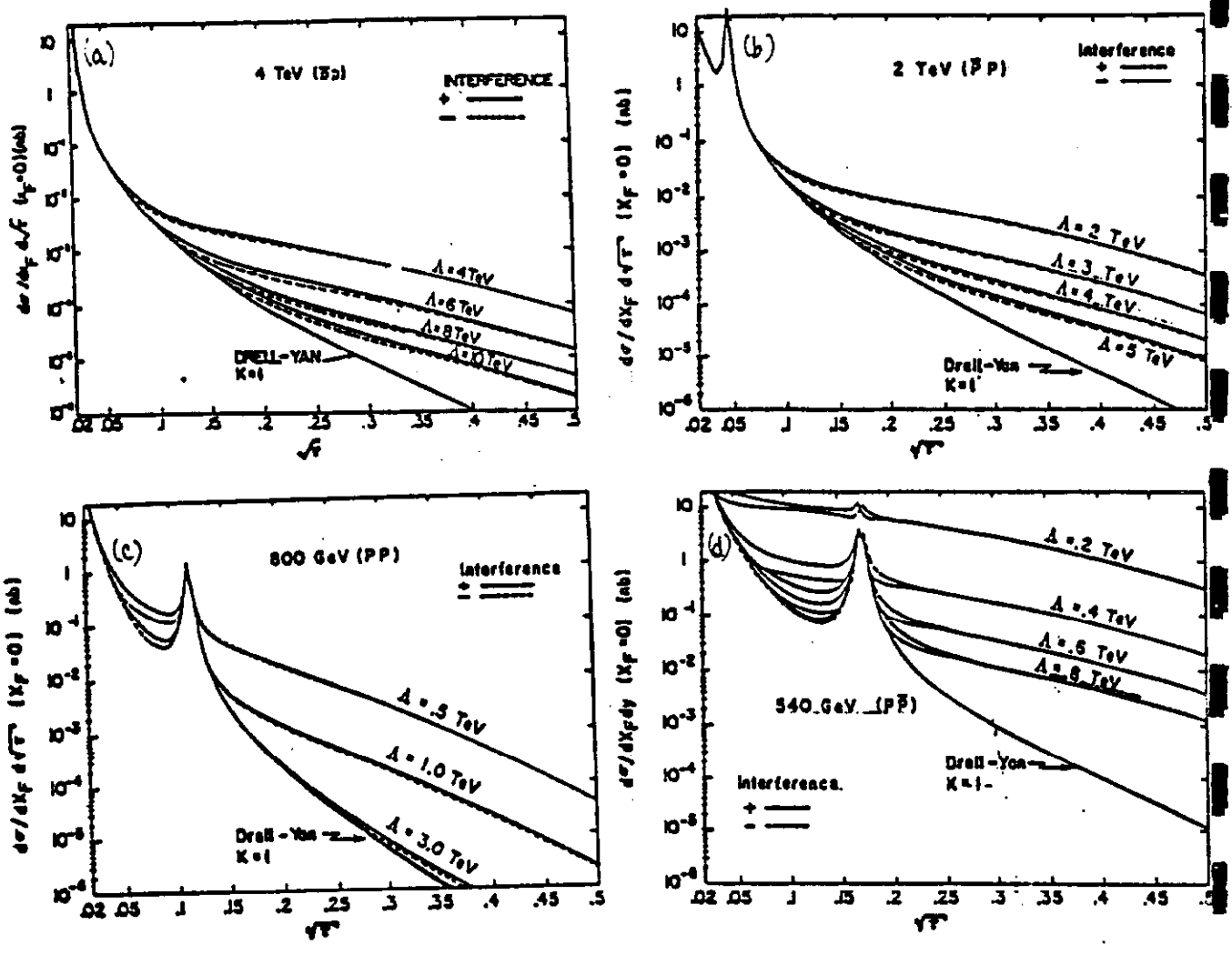

Fig. II-15. Deviations from lowest-order Drell-Yan yields induced by quark and lepton compositeness. (a) 4 TeV $\bar{p}p$ (b) 2 TeV $\bar{p}p$; (c) 0.8 TeV pp; (d) 0.54 TeV $\bar{p}p$. Here $\tau = m^2/s$.

number of events N accumulated in a collider run with integrated luminosity $\int dt \mathcal{L}$ at machine c.m. energy $\sqrt{s}$ will be given by

$$N=(c/\hat{s})F(\hat{s},s)\int dt\mathcal{L},$$

where $F(s,\hat{s})$ is a convolution over parton distribution functions in the colliding beams. For various values of c and for an assumed integrated luminosity of $\int dt\mathcal{L} = 10^{38}cm^{-2}$ characteristic of a DC run, we show in Fig. II-16 the value of the maximum subenergy $\sqrt{\hat{s}}$ for which a run at machine energy $\sqrt{s}$ will accumulate 100 events. We see again in a general way that the natural scale of subenergies to be explored at the DC is typically of order 0.5 to 1.5 TeV. This is superior to what can be reached with other colliders.

In summary, the mass scales on which the Dedicated Collider will be sensitive for various processes and new particles, as calculated above, is reviewed in Table II-14. The high physics interest and cost-effectiveness of the DC are apparent.

F. Uncertainties in Rate Estimates

In spite of the great efforts devoted to the study of deeply inelastic scattering and the extraction of structure functions, important ambiguities remain in the parton distributions. These are especially significant for small values of x and at all Q^2, and at large values of x for large Q^2. They arise both from the original parameterizations at modest Q^2 and from the QCD evolution to larger Q^2.

The parton distributions of Owens, Reya, and Duke that we have used for the illustrative calculations in this Section may be characterized as "gluon poor." For most purposes they may be regarded as providing conservative estimates of the cross sections. In the preliminary studies which led to this proposal we have found it useful to consider in addition the Baier, et al. distributions used in the Snowmass study, which represent the opposite extreme of "gluon rich" distributions. [For the Snowmass calculations, Λ=0.1 GeV was used; we take Λ=0.4 GeV, the value obtained by Baier, et al. in their fits. This makes little difference in the results.] Although we believe that reality is likely to lie closer to the gluon poor distributions, the more important point is that a comparison of the two distributions provides a measure of the uncertainty of any such calculations in light of current knowledge. It should also be remembered that the calculations we present are all lowest-order estimates subject to their own theoretical uncertainties.

Luminosity contours for the Baier, et al. distributions are shown in Fig. II-17. The relative importance of $u\bar{u}$ and gg collisions is different from what is displayed in Fig. II-16, but the energy dependence (as reflected in the slopes of the contours) is quite compatible. Thus the the absolute scale probed by a given machine is distribution-dependent, but the relative comparison among machines is rather insensitive to the parton distributions. The last point is

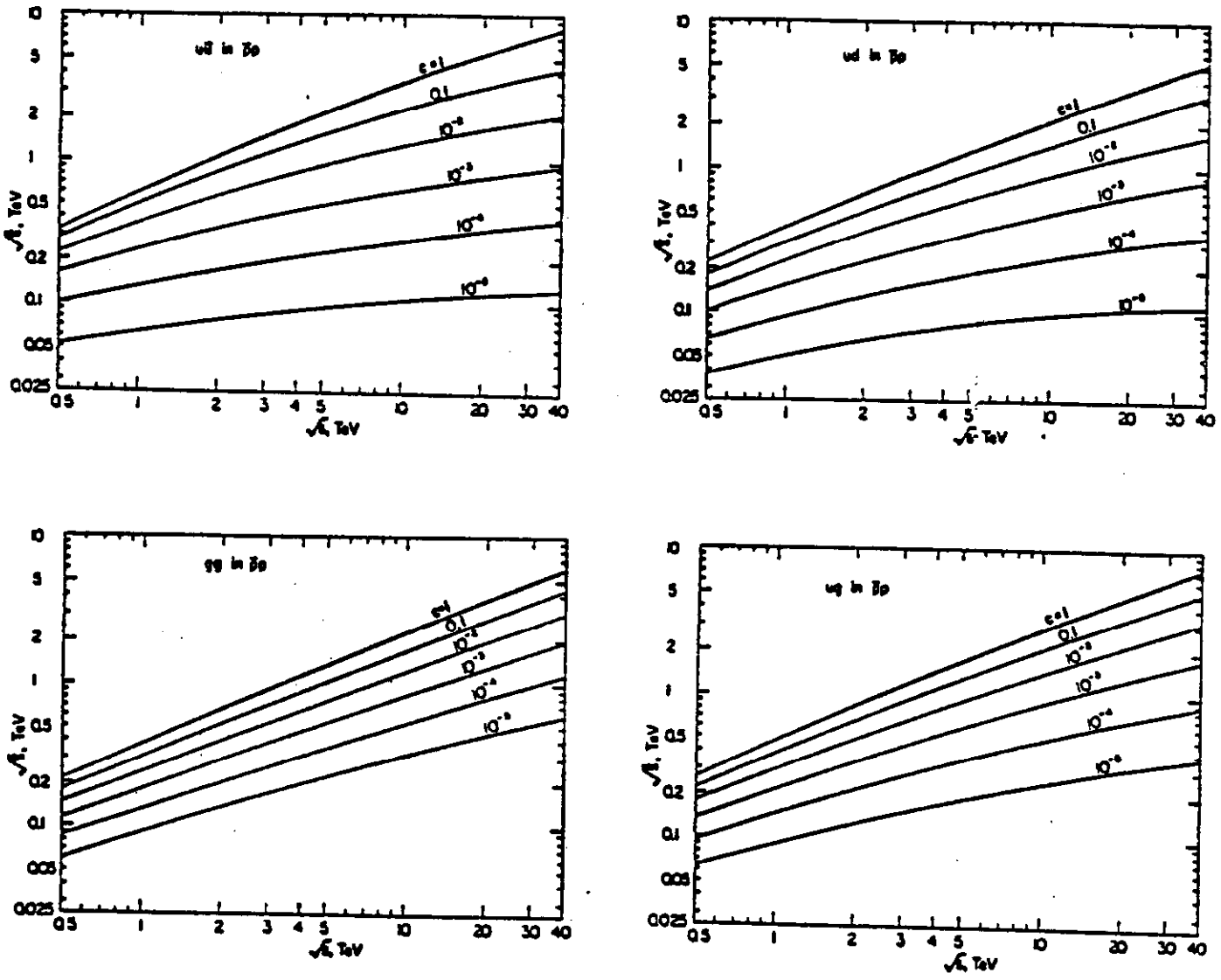

Fig. II-16. Contours in invariant mass of a hard collision yielding 100 events in running with integrated luminosity 10^{38}cm^{-2}, for hard-scattering cross sections $\sigma(\hat{s}) = c/\hat{s}$.

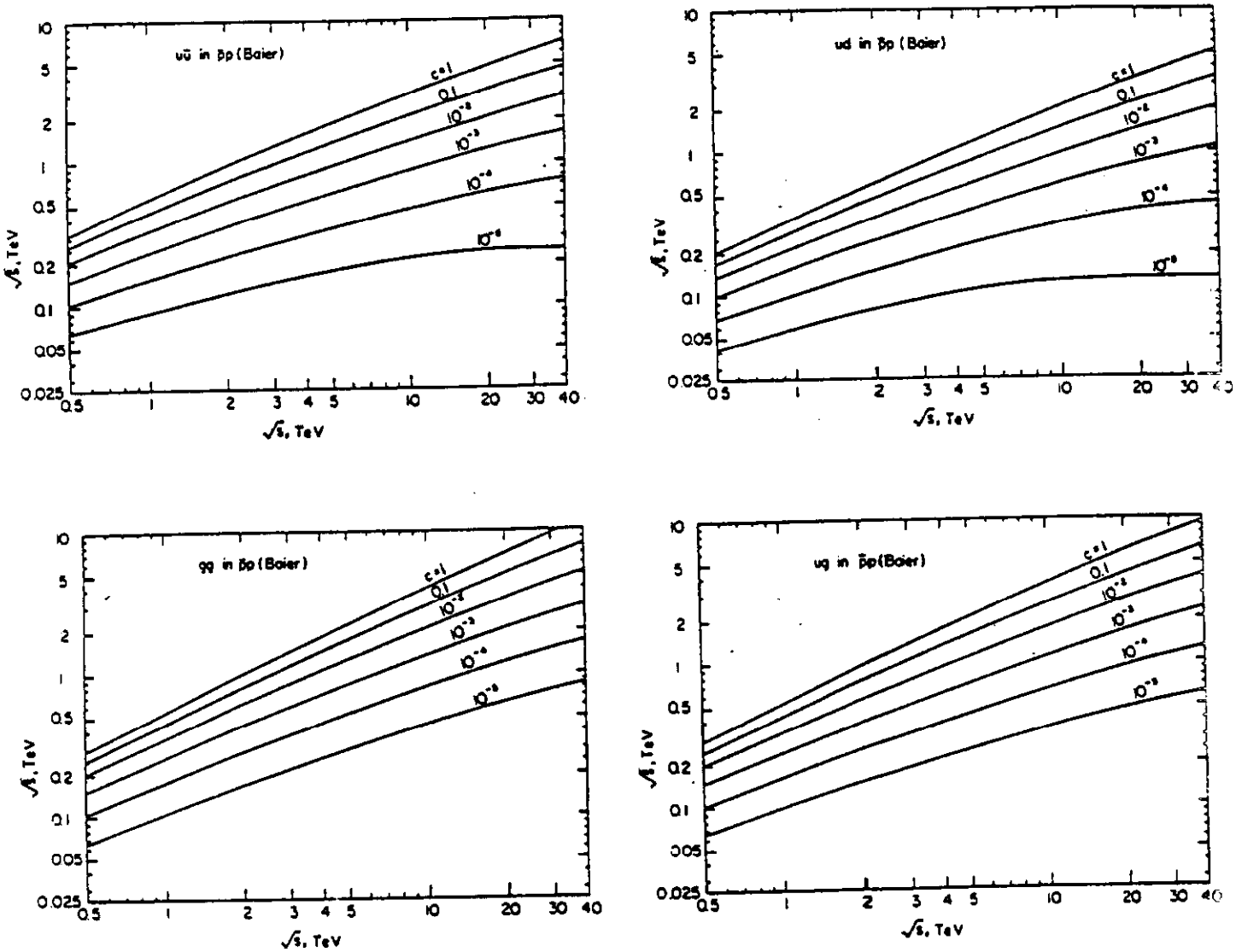

Fig. II-17 Contours in invariant mass of a hard collision yielding 100 events in running with integrated luminosity $10^{38}cm^{-2}$, for hard-scattering cross sections $\sigma(\hat{s})=c/\hat{s}$ (Baier parton distribution).

amplified by the Snowmass contour plots (Fig. 4, Snowmass, p. 96), and by Tables II-1A-II-14A, which provide crude assessments of machine capabilities according to the gluon rich distributions.

Table II-1. Number of standard model intermediate bosons anticipated in hadron-hadron colliders.

Collider	$\sqrt{s}$, TeV	$\int dt\mathcal{L}$, cm^{-2}	events W^+	W^-	Z°
DC($\bar{p}p$)	4.0	10^{38}	2×10^6	2×10^6	10^6
TeV I($\bar{p}p$)	2.0	10^{37}	10^5	10^5	60K
		10^{38}	10^6	10^6	600K
CBA(pp)	0.8	10^{38}	150K	80K	60K
		10^{40}	15×10^6	8×10^6	6×10^6
S$\bar{p}$pS	0.54	10^{37}	20K	20K	15K
		10^{38}	200K	200K	150K

Table II-2. Number of gauge boson pairs anticipated in hadron-hadron colliders.

Collider	$\sqrt{s}$, TeV	$\int dt\mathcal{L}$, cm^{-2}	events W^+W^-	W^-Z°	$Z^\circ Z^\circ$
DC($\bar{p}p$)	4.0	10^{38}	1.3K	700	370
TeV I($\bar{p}p$)	2.0	10^{37}	60	26	15
		10^{38}	600	260	150
CBA(pp)	0.8	10^{38}	8	1	1
		10^{40}	780	110	140
S$\bar{p}$pS	0.54	10^{37}	2	<1	<1
		10^{38}	22	3	3

Table II-1A. Number of standard model intermediate bosons anticipated in hadron-hadron colliders. [Baier distributions]

Collider	$\sqrt{s}$, TeV	$\int dt\mathcal{L}$, cm^{-2}	events W^+	W^-	Z^o
DC($\bar{p}p$)	4.0	10^{38}	15×10^6	15×10^6	8×10^6
TeV I($\bar{p}p$)	2.0	10^{37}	7×10^5	7×10^5	350K
		10^{38}	7×10^6	7×10^6	3.5×10^6
CBA(pp)	0.8	10^{38}	400K	250K	120K
		10^{40}	40×10^6	25×10^6	12×10^6
S$\bar{p}p$S	0.54	10^{37}	60K	60K	20K
		10^{38}	600K	600K	200K

Table II-2A. Number of gauge boson pairs anticipated in hadron-hadron colliders. [Baier distributions]

Collider	$\sqrt{s}$, TeV	$\int dt\mathcal{L}$, cm^{-2}	events W^+W^-	W^-Z^o	Z^oZ^o
DC($\bar{p}p$)	4.0	10^{38}	10K	5.1K	2.9K
TeV I($\bar{p}p$)	2.0	10^{37}	240	96	61
		10^{38}	2.4K	960	608
CBA(pp)	0.8	10^{38}	9	1.5	1.4
		10^{40}	920	150	140
S$\bar{p}p$S	0.54	10^{37}	2	.3	.3
		10^{38}	17	3	3

Table II-3. Maximum mass (in GeV/c^2) for production of 100 Higgs boson events in hadron-hadron colliders.

Collider	$\sqrt{s}$, TeV	$\int dt\mathcal{L}$, cm^{-2}	$M_H^{(max)}$ m_t=20	m_t=40	m_t=80
DC($\bar{p}p$)	4.0	10^{38}	135	175	220
TeV I($\bar{p}p$)	2.0	10^{37}	50	35	35
		10^{38}	100	115	80
CBA(pp)	0.8	10^{38}	55	50	45
		10^{40}	125	150	140
S$\bar{p}$pS	0.54	10^{37}	25	20	20
		10^{38}	40	35	40

Table II-4. Maximum quark mass (in GeV/c^2) for production of 100 quark-antiquark pairs in hadron-hadron colliders.

Collider	$\sqrt{s}$, TeV	$\int dt\mathcal{L}$, cm^{-2}	$M_q^{(max)}$
DC($\bar{p}p$)	4.0	10^{38}	320
TeV I($\bar{p}p$)	2.0	10^{37}	140
		10^{38}	220
CBA(pp)	0.8	10^{38}	85
		10^{40}	140
S$\bar{p}$pS	0.54	10^{37}	70
		10^{38}	95

Table II-3A. Maximum mass (in GeV/c^2) for production of 100 Higgs boson events in hadron-hadron colliders. [Baier distributions]

Collider	$\sqrt{s}$, TeV	$\int dt\mathcal{L}$, cm^{-2}	$M_H^{(max)}$ m_t=20	m_t=80
DC($\bar{p}p$)	4.0	10^{38}	170	340
TeV I($\bar{p}p$)	2.0	10^{37}	65	40
		10^{38}	120	215
CBA(pp)	0.8	10^{38}	70	45
		10^{40}	170	260
$S\bar{p}pS$	0.54	10^{37}	20	20
		10^{38}	50	35

Table II-4A. Maximum quark mass (in GeV/c^2) for production of 100 quark-antiquark pairs in hadron-hadron colliders. [Baier]

Collider	$\sqrt{s}$, TeV	$\int dt\mathcal{L}$, cm^{-2}	$M_q^{(max)}$
DC($\bar{p}p$)	4.0	10^{38}	395
TeV I($\bar{p}p$)	2.0	10^{37}	170
		10^{38}	240
CBA(pp)	0.8	10^{38}	110
		10^{40}	205
$S\bar{p}pS$	0.54	10^{37}	70
		10^{38}	95

Table II-5. Maximum mass (in GeV/c^2) for production of 100 $W'^{\pm}$ or Z'^0 gauge bosons in hadron-hadron colliders.

Collider	$\sqrt{s}$, TeV	$\int dt\mathcal{L}$, cm^{-2}	$M^{(max)}$
DC($\bar{p}p$)	4.0	10^{38}	1200
TeV I($\bar{p}p$)	2.0	10^{37}	500
		10^{38}	750
CBA(pp)	0.8	10^{38}	300
		10^{40}	400
S$\bar{p}$pS	0.54	10^{37}	200
		10^{38}	275

Table II-6. Maximum transverse momentum (in GeV/c) for production of 100 hadron jets per unit rapidity at $y_{c.m.} = 0$, per GeV/c transverse momentum, in hadron-hadron colliders.

Collider	$\sqrt{s}$, TeV	$\int dt\mathcal{L}$, cm^{-2}	$P_{\perp}^{(max)}$
DC($\bar{p}p$)	4.0	10^{38}	350
TeV I($\bar{p}p$)	2.0	10^{37}	175
		10^{38}	250
CBA(pp)	0.8	10^{38}	140
		10^{40}	210
S$\bar{p}$pS	0.54	10^{37}	95
		10^{38}	115

Table II-7. Maximum mass (in GeV/c^2) for single production of 100 η_T events in hadron-hadron collisions.

Collider	$\sqrt{s}$, TeV	$\int dt\mathcal{L}$, cm^{-2}	$M^{(max)}$
DC($\bar{p}p$)	4.0	10^{38}	640
TeV I($\bar{p}p$)	2.0	10^{37}	210
		10^{38}	340
CBA(pp)	0.8	10^{38}	160
		10^{40}	300

Table II-5A. Maximum mass (in GeV/c^2) for production of 100 $W'^{\pm}$ or Z'^0 gauge bosons in hadron-hadron colliders. [Baier]

Collider	$\sqrt{s}$, TeV	$\int dt\mathcal{L}$, cm^{-2}	$M^{(max)}$
DC($\bar{p}p$)	4.0	10^{38}	1180
TeV I($\bar{p}p$)	2.0	10^{37}	530
		10^{38}	730
CBA(pp)	0.8	10^{38}	260
		10^{40}	360
$S\bar{p}pS$	0.54	10^{37}	210
		10^{38}	270

Table II-6A. Maximum transverse momentum (in GeV/c) for production of 100 hadron jets per unit rapidity at $y_{c.m.} = 0$, per GeV/c transverse momentum, in hadron-hadron colliders. [Baier]

Collider	$\sqrt{s}$, eV	$\int dt\mathcal{L}$, cm^{-2}	$P_T^{(max)}$
DC($\bar{p}p$)	4.0	10^{38}	500
TeV I($\bar{p}p$)	2.0	10^{37}	225
		10^{38}	300
CBA(pp)	0.8	10^{38}	160
		10^{40}	235
$S\bar{p}pS$	0.54	10^{37}	100
		10^{38}	120

Table II-7A. Maximum mass (in GeV/c^2) for single production of 100 n_T events in hadron-hadron collisions. [Baier]

Collider	$\sqrt{s}$, TeV	$\int dt\mathcal{L}$, cm^{-2}	$M^{(max)}$
DC($\bar{p}p$)	4.0	10^{38}	1.4 TeV/c^2
TeV I($\bar{p}p$)	2.0	10^{37}	440
		10^{38}	760
CBA(pp)	0.8	10^{38}	280
		10^{40}	490

Table II-8. Maximum mass (in GeV/c^2) for production of 100 technihadron pairs in hadron-hadron collisions.

Collider	$\sqrt{s}$, TeV	$\int dt\mathcal{L}$, cm^{-2}	$M_T^{(max)}$ P_3(leptoquark)	P_6	$P_8(\eta_T)$
DC($\bar{p}p$)	4.0	10^{38}	260	330	345
TeV I($\bar{p}p$)	2.0	10^{37}	100	170	175
		10^{38}	170	240	240
CBA(pp)	0.8	10^{38}	80	100	100
		10^{40}	120	150	150

Table II-9. Maximum squark mass (in GeV/c^2) for production of 100 squark-antisquark pairs in hadron-hadron colliders.

Collider	$\sqrt{s}$, TeV	$\int dt\mathcal{L}$, cm^{-2}	$M_{\tilde{q}}^{(max)}$
DC($\bar{p}p$)	4.0	10^{38}	215
TeV I($\bar{p}p$)	2.0	10^{37}	100
		10^{38}	155
CBA(pp)	0.8	10^{38}	70
		10^{40}	120
S$\bar{p}p$S	0.54	10^{37}	45
		10^{38}	65

Table II-10. Maximum gluino mass (in GeV/c^2) for production of 100 gluino pairs in hadron-hadron colliders.

Collider	$\sqrt{s}$, TeV	$\int dt\mathcal{L}$, cm^{-2}	$M_{\tilde{g}}^{(max)}$
DC($\bar{p}p$)	4.0	10^{38}	400
TeV I($\bar{p}p$)	2.0	10^{37}	175
		10^{38}	275
CBA(pp)	0.8	10^{38}	110
		10^{40}	165
S$\bar{p}p$S	0.54	10^{37}	80
		10^{38}	110

Table II-8A. Maximum mass (in GeV/c^2) for production of 100 technihadron pairs in hadron-hadron collisions. [Baier distributions]

Collider	$\sqrt{s}$, TeV	$\int dt\mathcal{L}$, cm^{-2}	$M_T^{(max)}$ P_3(leptoquark)	P_6	$P_8(\eta_T)$
DC($\bar{p}p$)	4.0	10^{38}	340	500	500
TeV I($\bar{p}p$)	2.0	10^{37}	140	230	230
		10^{38}	210	320	320
CBA(pp)	0.8	10^{38}	100	150	150
		10^{40}	170	210	210

Table II-9A. Maximum squark mass (in GeV/c^2) for production of 100 squark-antisquark pairs in hadron-hadron colliders. [Baier]

Collider	$\sqrt{s}$, TeV	$\int dt\mathcal{L}$, cm^{-2}	$M_{\tilde{q}}^{(max)}$
DC($\bar{p}p$)	4.0	10^{38}	305
TeV I($\bar{p}p$)	2.0	10^{37}	120
		10^{38}	190
CBA(pp)	0.8	10^{38}	100
		10^{40}	170

Table II-10A. Maximum gluino mass (in GeV/c^2) for production of 100 gluino pairs in hadron-hadron colliders. [Baier]

Collider	$\sqrt{s}$, TeV	$\int dt\mathcal{L}$, cm^{-2}	$M_{\tilde{g}}^{(max)}$
DC($\bar{p}p$)	4.0	10^{38}	500
TeV I($\bar{p}p$)	2.0	10^{37}	240
		10^{38}	315
CBA(pp)	0.8	10^{38}	155
		10^{40}	215

Table II-11. Limits on a compositeness scale in the production of hadron jets.

Collider	$\sqrt{s}$, TeV	$\int dt\mathcal{L}$, cm^{-2}	Λ^{LH}, TeV
DC($\bar{p}p$)	4.0	10^{38}	3.0
TeV I($\bar{p}p$)	2.0	10^{37}	1.2
		10^{38}	1.5
CBA(pp)	0.8	10^{38}	1.2
		10^{40}	1.8
$S\bar{p}pS$	0.54	10^{37}	0.4
		10^{38}	0.6

Table II-12. Limits on a compositeness scale in Drell-Yan production of massive lepton pairs.

Collider	$\sqrt{s}$, TeV	$\int dt\mathcal{L}$, cm^{-2}	Λ^{LH}, TeV
DC($\bar{p}p$)	4.0	10^{38}	6.0
TeV I($\bar{p}p$)	2.0	10^{37}	2.5
		10^{38}	4.0
CBA(pp)	0.8	10^{38}	1.0
		10^{40}	2.0
$S\bar{p}pS$	0.54	10^{37}	0.8
		10^{38}	1.2

Table II-13. Maximum mass (in GeV/c^2) for production of 100 pairs of excited colored fermions in hadron-hadron colliders.

			$M^{(max)}$		
Collider	$\sqrt{s}$, TeV	$\int dt\mathcal{L}$, cm^{-2}	q^*_3	q^*_6	q^*_8
DC($\bar{p}p$)	4.0	10^{38}	325	440	455
TeV I($\bar{p}p$)	2.0	10^{37}	140	200	205
		10^{38}	220	285	290
CBA(pp)	0.8	10^{38}	85	105	110
		10^{40}	140	160	165

Table II-11A. Limits on a compositeness scale in the production of hadron jets. [Baier distributions]

Collider	$\sqrt{s}$, TeV	$\int dt\mathcal{L}$, cm^{-2}	Λ^{LH}, TeV
DC($\bar{p}p$)	4.0	10^{38}	2.2
TeV I($\bar{p}p$)	2.0	10^{37}	1.2
		10^{38}	1.6
CBA(pp)	0.8	10^{38}	1.2
		10^{40}	1.7
S$\bar{p}$pS	0.54	10^{37}	0.4
		10^{38}	0.6

Table II-12A. Limits on a compositeness scale in Drell-Yan production of massive lepton pairs. [Baier distributions]

Collider	$\sqrt{s}$, TeV	$\int dt\mathcal{L}$, cm^{-2}	Λ^{LH}, TeV
DC($\bar{p}p$)	4.0	10^{38}	5.5
TeV I($\bar{p}p$)	2.0	10^{37}	2.0
		10^{38}	3.0
CBA(pp)	0.8	10^{38}	1.2
		10^{40}	2.0
S$\bar{p}$pS	0.54	10^{37}	0.8
		10^{38}	1.2

Table II-13A. Maximum mass (in GeV/c^2) for production of 100 pairs of excited colored fermions in hadron-hadron colliders. [Baier]

				$M^{(max)}$	
Collider	$\sqrt{s}$, TeV	$\int dt\mathcal{L}$, cm^{-2}	q^*_3	q^*_6	q^*_8
DC($\bar{p}p$)	4.0	10^{38}	395	575	580
TeV I($\bar{p}p$)	2.0	10^{37}	170	255	260
		10^{38}	240	345	350
CBA(pp)	0.8	10^{38}	110	160	160
		10^{40}	205	215	220

Table II-14. Mass limits attainable in the DC for production of 100 events at $\int dt\mathcal{L} = 10^{38}cm^{-2}$.

Particle	Mass limit, GeV/c^2 DC	TeV I(10^{37})	CBA(10^{40})
Standard model:			
Higgs scalar	135-220	35-50	125-150
Heavy fermion	320	140	140
Jet pair mass	>700	350	420
New gauge bosons:			
W' or Z'	1200	500	400
Supersymmetric partners:			
squark	215	100	120
gluino	400	175	165
Technicparticles:			
octet	345	175	150
sextet	330	170	150
triplet	260	100	120
Higgs-like scalars			
P	640	210	300
P^8_0	400	110	230
Compositeness (hadron jets)			
LH scale	3000	1200	1800
RH scale	2500		

Table II-14A. Mass limits attainable in the DC for production of 100 events at $\int dt\mathcal{L} = 10^{38}cm^{-2}$. [Baier distributions]

Particle	Mass limit, GeV/c^2 DC	TeV I(10^{37})	CBA(10^{40})
Standard model:			
Higgs scalar	170-340	40-65	170-260
Heavy fermion	395	170	205
Jet pair mass	1000	450	470
New gauge bosons:			
W' or Z'	1200	530	360
Supersymmetric partners:			
squark	300	120	170
gluino	500	240	215
Technipartícles:			
octet	500	230	210
sextet	500	230	210
triplet	340	140	170
Higgs-like scalars			
P	1400	440	490
P^0	960	190	300
Compositeness (hadron jets)			
LH scale	2200	1200	1700
RH scale	1800		

G. Electron-Proton Physics

In Phase I of an ep physics facility at the Dedicated Collider (10 GeV electrons (positrons) on 2 TeV protons (antiprotons)) we enter a new kinematical region where electromagnetic and weak interactions become of comparable strength. The effects of the t channel exchange of W's and Z's are seen clearly, and detailed studies of both $SU(2)\times U(1)$ and QCD are possible. An ep facility provides complementary physics to both the e^+e^- physics of LEP and SLC and the $p\bar{p}$ physics we have been discussing. In addition, we are able to search for possible modifications to the standard model--detection of right-handed currents, neutral heavy leptons, leptoquarks, quark substructure, and composite model interactions.

With the envisioned Phase II (40 GeV electron ring) we could concentrate on extending the search for new phenomena and heavy particles well beyond those accessible even at LEP II.

Below we will discuss the physics opportunities at an ep facility operating at $s = 8\times10^{3}\,GeV^2$ with an integrated luminosity of $5\times10^{38}\ cm^{-2}$ in a standard 1 yr run.

1. Standard Physics: QCD

An initial program at the ep facility will of course study the total cross sections and structure functions. Knowledge of the structure functions at small x and large Q^2 will provide valuable information for use in the study of $p\bar{p}$ physics. The cross section for the one photon contribution which dominated the neutral process can be written

$$d\sigma = \frac{4\pi\alpha^2}{Q^2}\left[1 - Q^2/sx + 1/2\,(Q^2/sx)^2\right] F_2(x,Q^2)\,\frac{dx}{x}\,\frac{dQ^2}{Q^2}\,.$$

Since all s dependence comes from the bracketed factor which only varies by a factor of 2 over the whole kinematic range ($0<Q^2<sx$), we conclude that although increasing s increases the accessible Q^2 at a given x, it does not appreciably increase the yield of events in a given accessible x and Q^2 bin.

The range of Q^2 - x which is accessible with the ep collider is shown in Fig. II-18.

Another aspect of standard QCD measurements which will complement the $p\bar{p}$ mode is the ability in an ep machine to correlate the energy and momentum of the struck quark with the properties of the resulting jet. The kinematic constraints obtained from observing the outgoing lepton in neutral current reactions allows a study of the dressing of the quark into the jet of hadrons and a fuller understanding of the mechanism of jet broadening for energetic quarks.

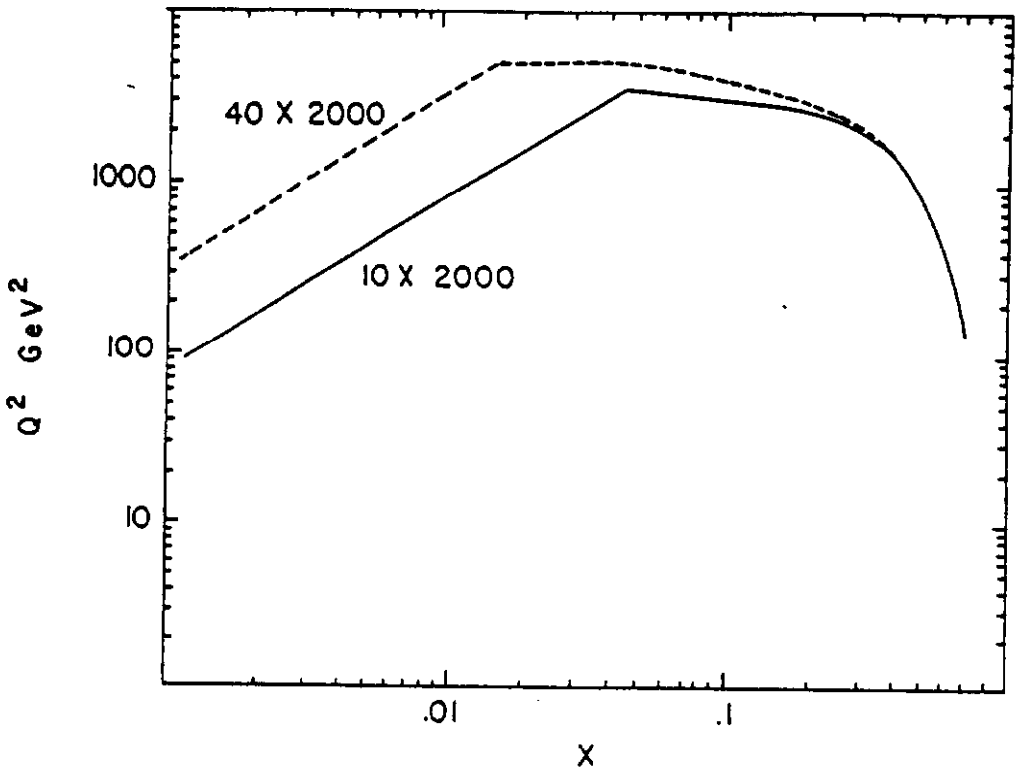

Fig. II-18 . The Q^2-x contours with bin sizes $dx/x = .1$ and $dQ^2/Q^2 = .1$ and yielding per bin greater than 100 events/yr. in a 1 yr. run with integrated luminosity $5 \times 10^{38} cm^{-2}$.

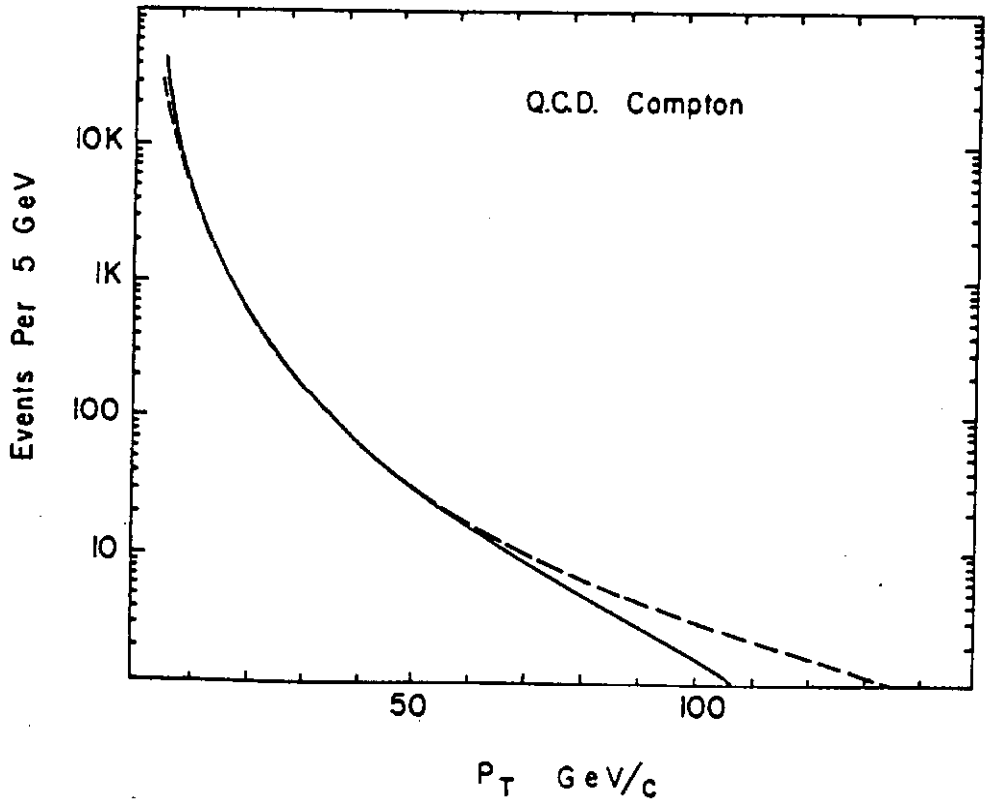

Fig. II-19 . Expected yield of large tranverse momentum events anticipated in the QCD Compton process $\gamma + q \rightarrow g + q$ for a run of $\int dt\mathcal{L} = 5 \times 10^{38} cm^{-2}$ in 10 GeV on 2 TeV ep collisions.

The study of the high-energy QCD Compton process depicted in Fig. II-19 provides a method to study gluon fragmentation. This process, where a high-energy photon scatters off a quark in the proton creating a wide angle gluon jet and a wide angle quark jet, is essentially the inverse of one of the mechanisms thought responsible for direct photon production in hadron-hadron collisions. In the kinematic regime where the final quark and gluon jet emerge with a large p_t (say $p_t > 15$ GeV), the cross section calculation should be fairly reliable, and hence measurements of the process will serve as powerful tests of QCD. The ratio of the QCD Compton cross section over the QED Compton cross section (which would have a high p_t photon against a quark jet) serves as a direct and independent measurement of α_s. Correlations are expected between the plane defined by the quark and gluon jets and the polarization vector of the virtual photon. These correlations serve to directly test the form of the quark gluon coupling. For example, this angular correlation is expected to have the opposite sign from the analogous correlation predicted for the QED Compton process.

The QCD Compton process being a low Q^2 process with two high p_t jets will produce events which can easily be experimentally distinguished from normal neutral current events consisting of a single large p_t jet and a large Q^2 scattered electron. However, the light-quark photon-gluon fusion contribution produces a background with the same general topology as the QCD Compton process. It is possible to suppress the photon-gluon fusion process relative to the QCD Compton process by demanding that the parton within the incident proton which collides with the virtual photon has a large fraction of the incident proton momentum. A lower cut on parton energy fraction suppresses the gluon initiated process relative to the quark initiated process since gluons tend to carry a much smaller fraction of the proton momentum than the valence quarks. Energy balance can be used to find ξ, the fraction of momentum of the incident proton carried by the parton which collided with the virtual photon for a given two-jet event. The cut $\xi > 0.6$ reduces the photon-gluon background to about 10%.

Virtual photoproduction processes provide an excellent source for heavy quark production. For example, the expected top quark yield as a function of quark mass for the assumption of vector meson dominance is shown in Fig. II-20. A minimum electron tagging angle of 3° is used and the photoproduction cross section is scaled by $(m_c/m_t)^2$ from the known charm photoproduction cross section. Finally, a high q^2 cutoff of the vector meson form factor is included. The virtual photoproduction rates for D^0, B, t (m = 20 GeV) and t(m = 50 GeV) are summarized in Table II-15. It should be added that these events are easy to recognize.

Finally, as shown in Fig. II-21, the photon-gluon fission process allows for the production of 100 events for top quark masses up to 80 GeV in Phase I and 100 GeV in Phase II.

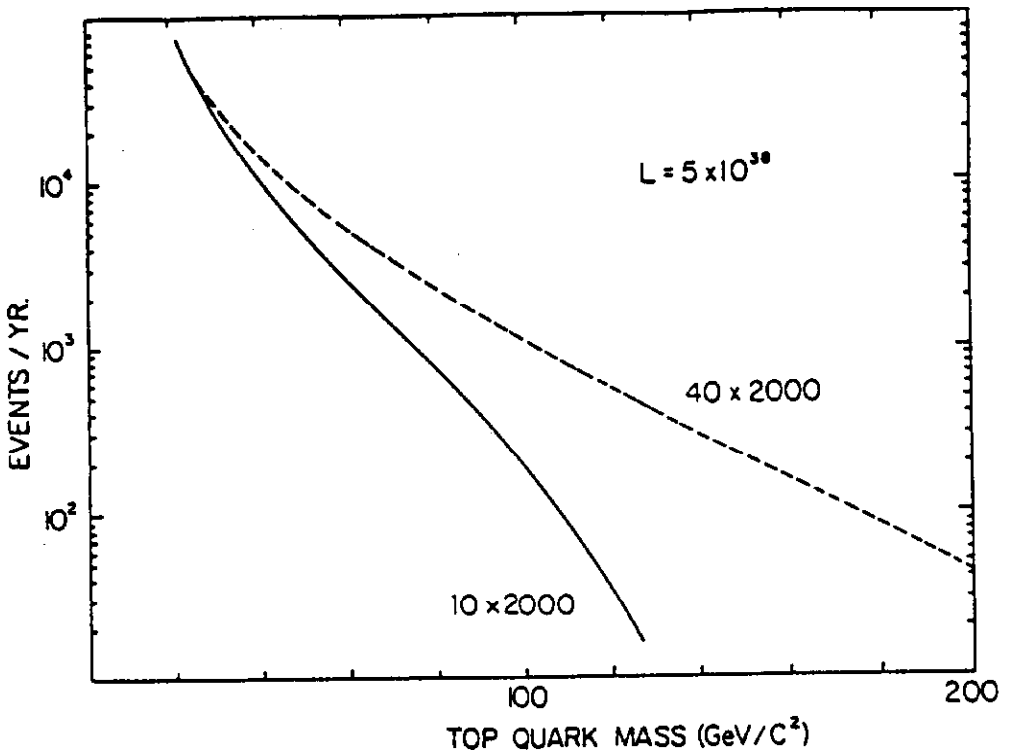

Fig. II-20. Yield of top quarks anticipated in ep collisions for an integrated luminosity of $\int dt\mathcal{L} = 5 \times 10^{38} cm^{-2}$.

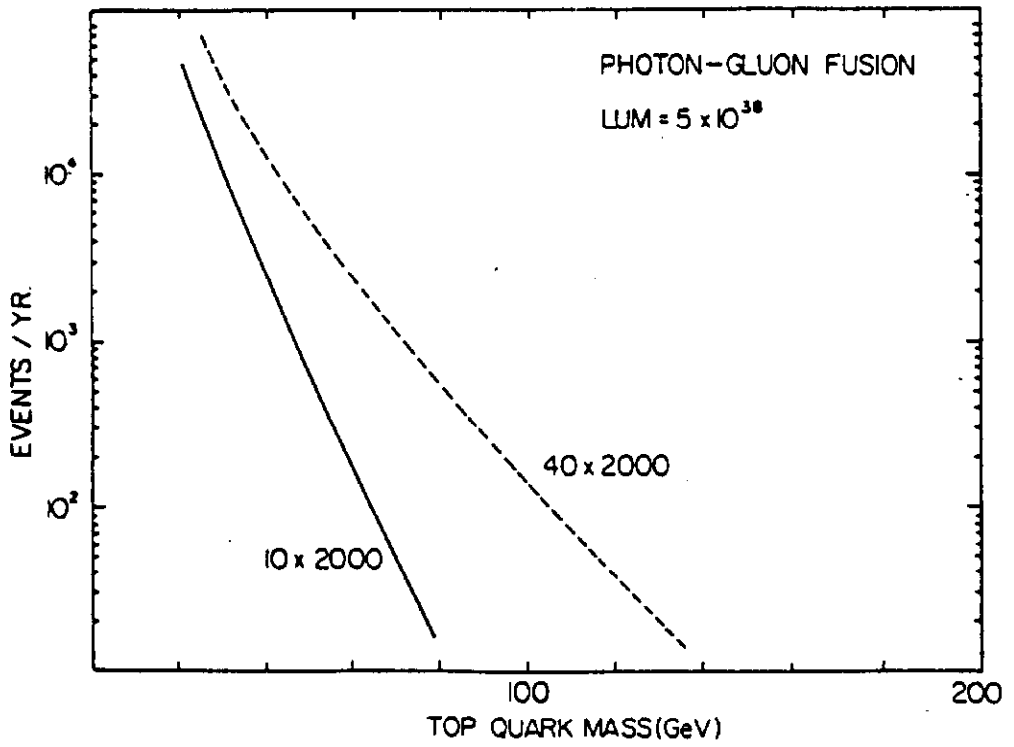

Fig. II-21. Top quark pair production by photon-gluon fusion for $\int dt\mathcal{L} = 5 \times 10^{38} cm^{-2}$.

2. Standard Physics: Electroweak Phenomena

The asymmetry, A, in low Q^2 electron proton scattering observed at SLAC gave the first compelling evidence for the existence of weak and electromagnetic interferences in neutral current processes.

$$A = \frac{\sigma_{e-} - \sigma_{e+}}{\sigma_{e-} + \sigma_{e+}} = \frac{2\sqrt{2}\, G_F}{e^2} \frac{Q^2}{1+Q^2/m^2} \times$$

$$\frac{1 - (1-y)^2}{1 + (1-y)^2} \frac{xF_3^{\text{Interference}}(x,Q^2)}{F_2^{em}(x,Q^2)} .$$

This effect should reach ~25% in the Phase I ep collider. The major contribution of ep scattering for the neutral currents will be as a test of the standard model in the extreme spacelike region. Deviations from the expected Q^2 dependence of the asymmetry parameter A could signify the presence of additional neutral vector bosons more massive than the Z^0.

In the normal charged current process, an electron will scatter from a quark via a W exchange leaving a neutrino (which will escape detection) and a wide angle current jet in the final state. The evolution of the charged current propagator allows a measurement of the mass of the W to within ±4 GeV even with a 20% uncertainty in the ep luminosity.

By fitting the shape of the W propagator, we will be sensitive to the possible effects of multiple W's. The mass and coupling of the standard W will have been determined from the $S\bar{p}pS$ collider experiments. Using these as inputs to the fit of the effective charged-current propagator determined in the ep collider, the presence of a second W can be determined up to a mass of 400 GeV.

3. Extensions of the Standard Model

We have seen that the $p\bar{p}$ collider at DC will be sensitive to a second W up to a mass ~1200 GeV. In extensions of the standard model, one very appealing idea is that parity is restored at sufficiently high energies and therefore a W' which couples to right-handed electrons would exist. If such a W' is found, the ep collider could be invaluable in determining the handedness of W'. If we assume that the right-handed W couples to right-handed leptons and quarks in a fashion analogous to the left-handed couplings of the standard W and that the right-handed ν_R is sufficiently light to give no additional kinematic suppression to these processes, then we can search for the presence of a right-handed charged current by looking for a Q^2 dependence in R_D (the ratio of charged current events for right-handed polarized electrons to charged

current events for left-handed polarized electrons). The limit accessible to the ep facility in Phase I is 600 GeV. We may alternately ask, to what level would the ep collider be sensitive to the existence of the neutral heavy lepton which is the final leptonic state in a right-handed charged current coupling. If we assume that the right-handed charged current coupling is identical in strength to the left-handed coupling, as shown in Fig. II-22, we would be sensitive to masses up to 200 GeV in Phase I and 400 GeV in Phase II.

4. Other Possibilities

a) Technicolor

Models which construct quarks and leptons from elementary constituents or in which there is a new strong interaction predict the existence of leptoquarks with masses possibly in the vicinity of hundreds of GeV and widths which might be narrow. An ep collider offers unique advantages in searching for the existence of massive leptoquarks and leptogluons since they can be produced directly in the s-channel, and will produce peaks in the neutral current structure functions at an $x = M^2/s$. Production of scalar leptoquarks is expected to be very low owing to the nature of their coupling. Vector leptoquark yields might be copious, however, if the lepton-quark interaction scale is on the order of 1 TeV. Figure III-23 gives the expected rates for our standard ep run. It assumes the following production cross sections.

$$\sigma = \frac{4\pi^2 \alpha_{LQ}}{M_{LQ}^2} \, xu(x) \Bigg|_{x = \frac{M_{LQ}^2}{s}}$$

$$\sigma = 4\pi^2 \alpha_s \frac{M_{Lg}^2}{\Lambda^4} \, xg(x) \Bigg|_{x = \frac{M_{Lg}^2}{s}} .$$

b) Supersymmetry

In models with supersymmetry at the TeV scale each of the usual particles has a partner with spin differing by one half and a mass below a few hundred GeV. Although the $p\bar{p}$ collider will in general be more sensitive to these superpartners, an ep collider would produce 100 squark pairs/yr for masses up to 55 GeV in Phase I and 85 GeV in Phase II. The production rate for squark pairs for an integrated luminosity of 5×10^{38} is shown in Fig. II-24.

c) Quark Substructure and Compositeness

Other modifications to the standard model which could appear in ep interactions would be the observation of quark substructure. The

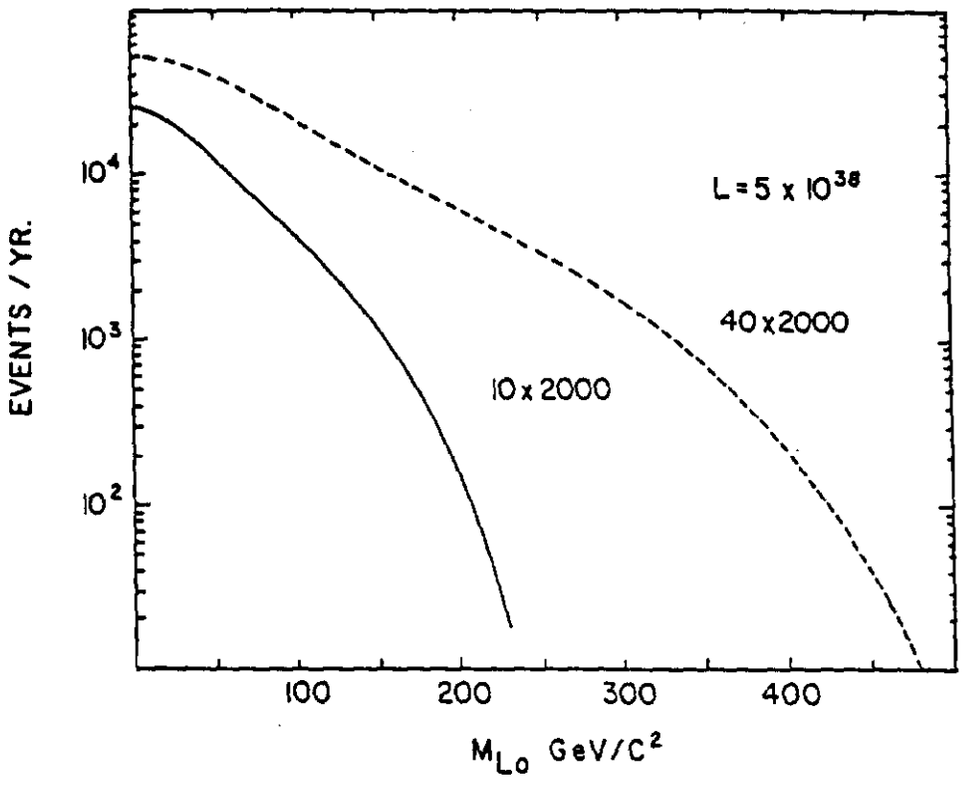

Fig. II-22. Sensitivity of the ep collider to neutral heavy leptons coupled to the electron with a right-handed interaction of universal Fermi strength.

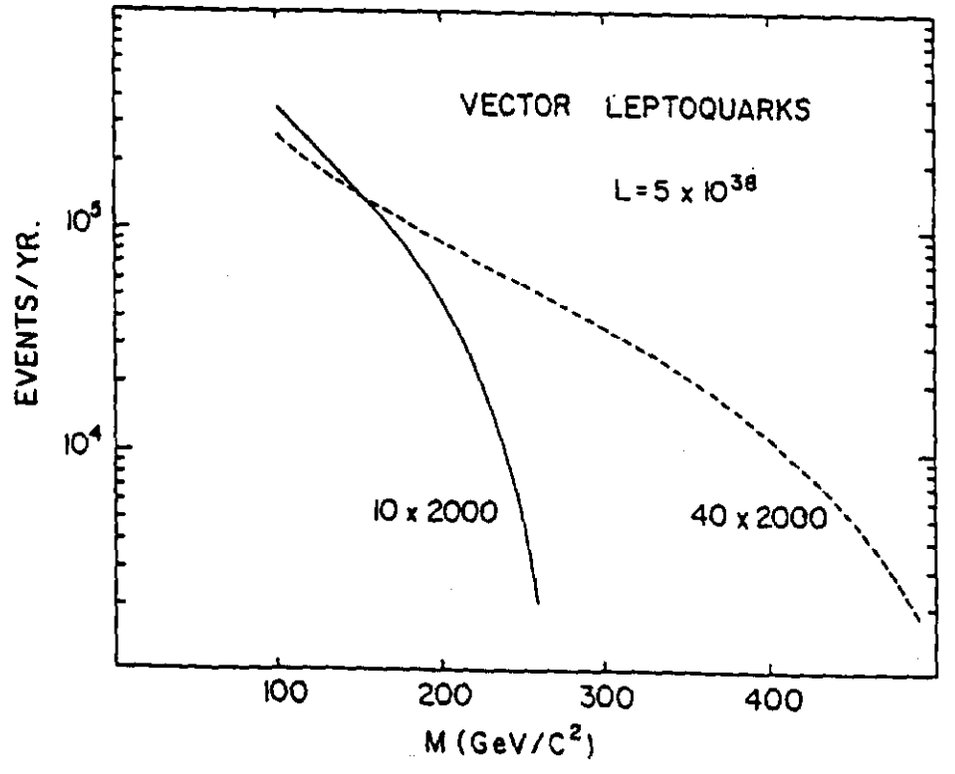

Fig. II-23. Yield of vector leptoquarks in a run of $\int dt\mathcal{L} = 5 \times 10^{38} cm^{-2}$ in ep colliders.

electron-proton collider will allow measurements of the nucleon structure function up to Q^2 = 10,000 GeV at s = $8\times10^4 GeV^2$ and searches for power law contributions to scale breaking at mass scales up to 500 GeV. Such power law contributions could be an indication of quark substructure. If quark substructure is present, it should manifest itself through the existence of events which look dramatically different from ordinary ep events.

If quarks and leptons are constructed from similar building blocks, one can anticipate new interactions where quark-lepton scattering occurs by constituent exchange rather than by photon exchange. Such a contact interaction will interfere with the normal neutral current amplitude to create a deviation which is approximately linear in q^2:

$$\frac{d\sigma/dQ^2}{d\sigma/dQ^2}_{\Lambda=\infty} = 1 \pm \frac{A^{-1/2}Q^2}{\Lambda^2}$$

where Λ is the compositeness scale of quarks and leptons and A is of order one. Figures II-25 and II-26 show the ratio of the yield of neutral current events with q^2/q_0^2 when a contact term is present over the yield of neutral current events when a contact term is absent. The high-energy ep machine allows a considerable extension in q^2. Figure II-27 compares the statistical significance of the contact effect as a function of the compositeness scale $\alpha\Lambda^2$ in units of 10^5 GeV^2. The vertical coordinate is in standard deviations.

5. Summary

We summarize in Table II-16 the physics capabilities of an ep collider operating at s = 8×10^4 GeV^2 with an integrated luminosity of $5\times10^{38}cm^{-2}$.

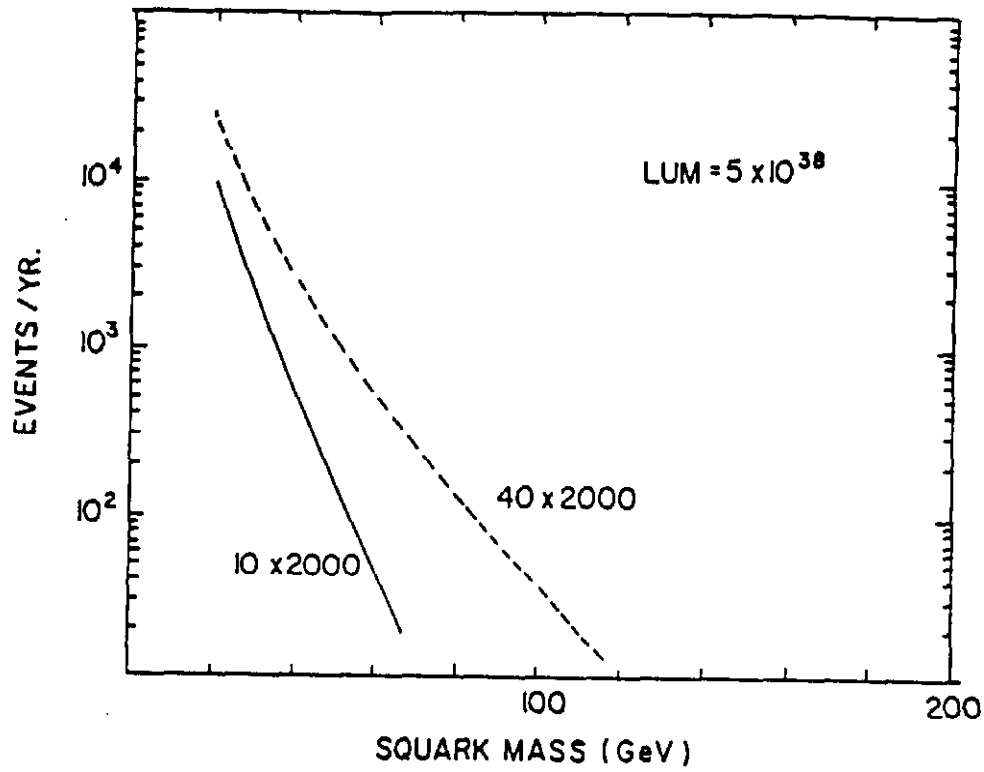

Fig. II-24. Expected yield of squark pairs with integrated luminosity 5 x 10^{38}cm^{-}

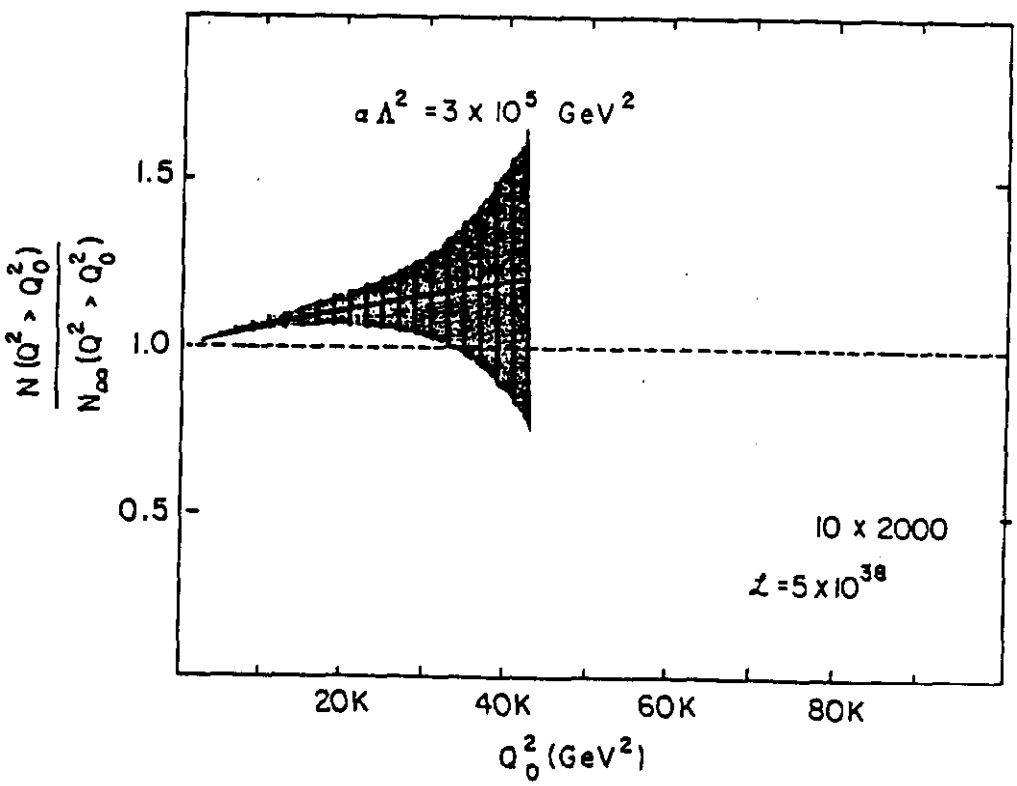

Fig. II-25. Ratio of the yield of neutral current events with $Q^2>Q_o^2$ in the presence of a contact interaction to those expected in the conventional picture, for the 10 GeV on 2 TeV ep collider. The error band is calculated for a run of integrated luminosity $\int dt \mathcal{L}$ = 5 x 10^{38}cm^{-2}

Table II-15. Virtual Photoproduction of Heavy Quark States

	Assumed Cross Section	Expected Yield *
1) $\gamma^* \to D^0\bar{D}^0$	500 nb $(1 - \frac{12\ GeV}{\nu})$	1.0×10^7
2) $\gamma^* \to B\bar{B}$	27 nb $(1 - \frac{68\ GeV}{\nu})$	7.4×10^5
3) $\gamma^* \to t\bar{t}$ (20 GeV top)	7 nb $(1 - \frac{893\ GeV}{\nu})$	1.5×10^5
4) $\gamma^* \to t\bar{t}$ (50 GeV top)	1.2 nb $(1 - \frac{5431\ GeV}{\nu})$	1.1×10^4

*Yield for an integrated luminosity of $5\times10^{38}cm^{-2}$ 10 on 2000 GeV ep collisions.

Table II-16. Sensitivity of various processes for $s = 8\times10^4 GeV^2$ and $\int dt\mathcal{L} = 5\times10^{38}cm^{-2}$

Process	Limit
QCD tests	$Q^2_{max} \simeq 10{,}000\ GeV^2$
W width	$\Delta M_W = 4$ GeV
W'	$m_{W'} = 400$ GeV
Right-handed W	$m_{W_R} = 600$ GeV
Top quark production ($m_t = 50$ GeV)	6,000 events/yr
Neutral Heavy Lepton	$m_{L^0} = 200$ GeV
Vector Leptoquark ($m_{L\bar{Q}} = 250$ GeV)	4,000 events/yr
Squark production (100ev/yr)	55 GeV
Quark substructure	4.0×10^{-17}cm
Composite eq interaction	$\Lambda > 6$ TeV

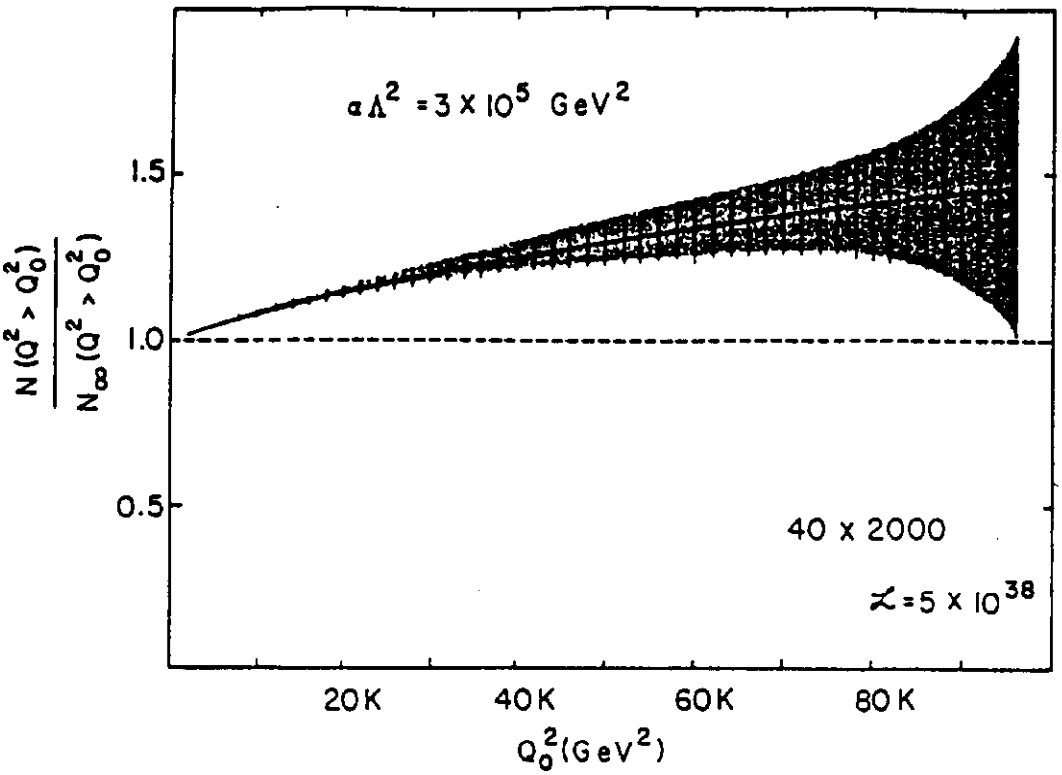

Fig. II-26. Ratio of the yield of neutral current events with $Q^2 > Q_0^2$ in the presence of a contact interaction to those expected in the conventional picture, for the 40 GeV on 2 TeV collisions. The error band is calculated for a run of integrated luminosity $\int dt\mathcal{L} = 5 \times 10^{38} cm^{-2}$

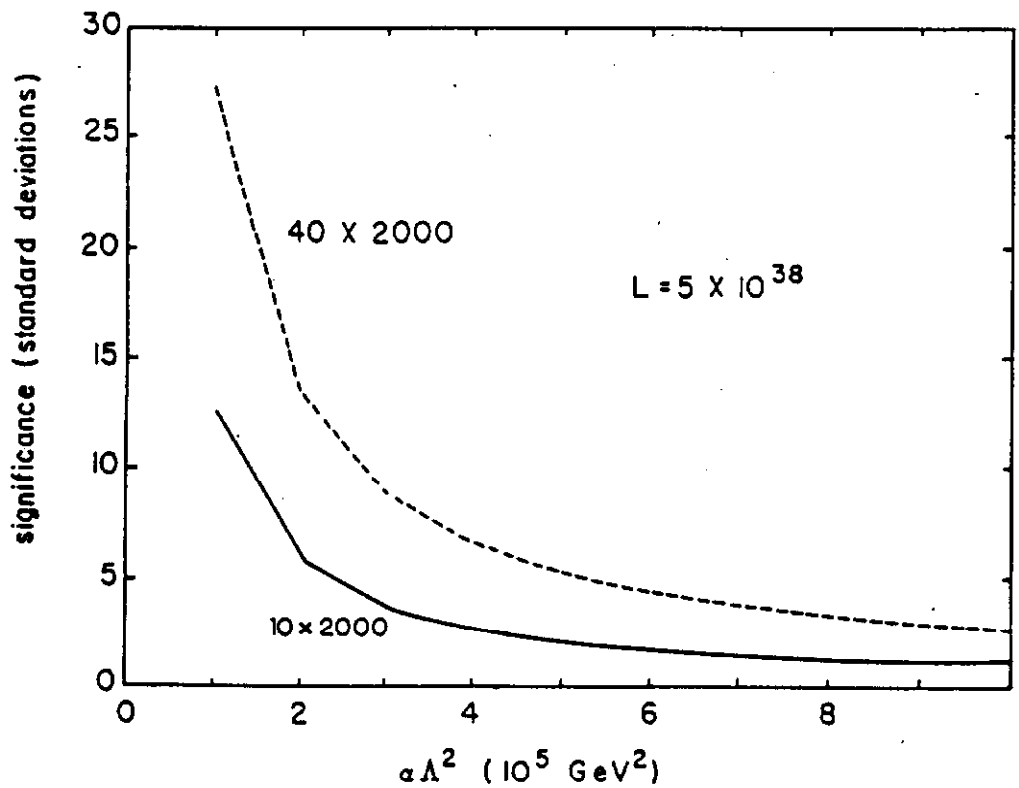

Fig. II-27. Statistical significance of the contact term's effect upon neutral current cross sections as a function of the compositeness scale for a run of $\int dt\mathcal{L} = 5 \times 10^{38} cm^{-2}$ in ep colliders.